



## Design and economic evaluation of a novel amine-based CO<sub>2</sub> capture process for SMR-based hydrogen production plants

Muhammad Zubair Shahid, Jin-Kuk Kim \*

Department of Chemical Engineering, Hanyang University, 222 Wangsimni-ro, Seongdong-gu, 04763, Seoul, Republic of Korea



### ARTICLE INFO

Handling Editor: Cecilia Maria Villas Boas de Almeida

**Keywords:**  
CO<sub>2</sub> capture  
Hydrogen plant  
Amine solvent  
Process design  
Economic analysis

### ABSTRACT

Chemical absorption using amine solvents is the most commercially recognized technology to capture CO<sub>2</sub> from the SMR-based hydrogen production plant. Most studies focused on the use of PSA inlet or tail gas streams to remove CO<sub>2</sub> using MDEA solvent which is limited to about 60% of total plant CO<sub>2</sub> emitted. Whilst the capture of a flue gas stream has been reported via the MEA solvent to remove 90% CO<sub>2</sub> yet at relatively higher costs. A systematic investigation is required to identify the cost-effective use of the absorption processes when multiple positions are available for CO<sub>2</sub> capture. In this study, multiple cases of the CO<sub>2</sub> absorption process have been evaluated using MEA or MDEA solvents. Especially, a novel design for the simultaneous removal of CO<sub>2</sub> from the flue gas of a reformer and the PSA inlet gas stream is proposed and its techno-economic benefits are examined. For this purpose, the rate-based model has been implemented in the MATLAB environment to simulate the absorption process, whereas the solvent regeneration energy and the capital and operating costs of the main equipment have been estimated using the correlations taken from the literature. The new system based on the sequential reuse of MEA solvent for two streams is found to be the most economic process to remove 99% of total plant CO<sub>2</sub>. The annualized cost of the proposed system is found 17.9% less in comparison to the best relevant conventional studied system of simultaneously removing CO<sub>2</sub> from the PSA inlet and reformer flue gas streams using MEA and MDEA solvents.

### 1. Introduction

Anthropogenic activities have already increased global warming from 0.8 °C to 1.2 °C above the pre-industrial levels. It is expected to reach 1.5 °C in the next few decades if it is continued at the same rate. In the Paris agreement (COP21), an international treaty on climate change was agreed to appreciably reduce CO<sub>2</sub> emissions so that global warming may not exceed 1.5 °C or at least remains well below 2 °C. To meet this goal, most countries have targeted to achieve net-zero emissions by mid-century (The-Paris-Agreement-2021). However, according to the report published by Intergovernmental Panel on Climate Change (IPCC) in 2018, the current efforts of CO<sub>2</sub> mitigation are inadequate to even achieve the target of 2 °C which otherwise may result in worse climate change (IPCC, 2018). Therefore, more serious efforts are required for the radical and urgent transition in energy technology to establish a clean energy production system (IEA, 2020).

Hydrogen is deemed to be the practical alternative to fossil fuels since it can be used in any place where fossil fuels are consumed from the industrial sector to the transportation sector (van der Spek et al.,

2022). A variety of technologies are available to produce green hydrogen via water splitting and dehydration of the hydrogen carrier molecules (Atilhan et al., 2021). Green hydrogen production has been facing technological and economical challenges that made yet it practically hard to be commercially established soon (Noussan et al., 2021). On the other hand, grey hydrogen production capacity is estimated at about 120 MT/year (Capurso et al., 2022) and is considered to be a cause of CO<sub>2</sub> emissions, contributing to about 2% of global warming among the energy sectors (van der Spek et al., 2022). Nevertheless, with the transformation of grey hydrogen production to blue hydrogen via the retrofitting of the plant with a CO<sub>2</sub> capture facility the CO<sub>2</sub> emissions can significantly be reduced (Soltani et al., 2021). The main barrier in this transformation is the cost of hydrogen production which sufficiently increases when the CO<sub>2</sub> capture facility is coupled. For instance, in Europe, currently, to produce blue hydrogen via the steam-methane-reforming (SMR) process, the CO<sub>2</sub> avoidance cost is estimated in the range of €50–70/ton<sub>CO<sub>2</sub></sub> (Hulst, 2019). However, it is to note that many countries want to raise the tax penalty on CO<sub>2</sub> emissions which eventually will shrink the cost gap between blue and grey

\* Corresponding author.

E-mail address: [jinkukkim@hanyang.ac.kr](mailto:jinkukkim@hanyang.ac.kr) (J.-K. Kim).

hydrogen production (Hulst, 2019). Therefore, one of the most practical pathways for establishing clean energy technology and achieving the net-zero emissions goal by mid-century is the production of blue hydrogen. Currently, hydrogen production via steam-methane-reforming (SMR) is the most commonly used technology to contribute more than 80% of the total produced hydrogen (Younas et al., 2022). It is also considered the most economical technology thereby the SMR process is evaluated to produce blue hydrogen via coupling with the carbon capture utilization and storage (CCUS) system. It is inferred that the economy of blue hydrogen production can be further improved by increasing the effective utilization of captured CO<sub>2</sub> (Ali Khan et al., 2021).

In the conventional steam-methane-reforming (SMR) process, methane is converted into synthesis gas via the catalytic reforming reaction over high temperature (630–930 °C) and mild to high pressure (5–25 bar) (Song et al., 2022). Further, the synthesis gas is reacted with steam in a water-gas shift reaction which increases the yield of hydrogen and converts carbon monoxide into carbon dioxide gas. This reaction is often operated in two stages, first at a high temperature (320–360 °C) followed by a lower temperature (190–250 °C) where the pressure is maintained in the range of 10–60 bar. This hydrogen-rich shifted synthesis gas then enters the pressure-swing-adsorption (PSA) unit to separate hydrogen gas from CO<sub>2</sub> and remaining methane and other impurities. The gas stream contains CO<sub>2</sub> and hydrocarbons are recycled to the gas reforming furnace to generate heat where the CO<sub>2</sub> is exhausted along with the produced flue gases (Voldsgaard et al., 2016). To retrofit the CO<sub>2</sub> capture facility with the SMR plant, the CO<sub>2</sub>-capture plant can be integrated with three possible streams: shifted synthesis gas, PSA tail gas, and the reformer flue gas. About 60% of the total plant CO<sub>2</sub> is produced in the reforming reaction whereas the rest 40% of CO<sub>2</sub> is produced during combustion in the furnace of the reforming section (Voldsgaard et al., 2016). Thereby the retrofitting of the CO<sub>2</sub> capture facility to the shifted gas or PSA tail gas streams cannot result in the overall capturing of more than about 60% CO<sub>2</sub> (Voldsgaard et al., 2016). To capture all the produced CO<sub>2</sub> either a single high-capacity CO<sub>2</sub> capture facility is required for the flue gas stream or the dual CO<sub>2</sub> capture facilities using any of the shifted synthesis gas streams or the PSA tail gas stream along with the flue gas stream option (Voldsgaard et al., 2016).

Several CO<sub>2</sub> capture technologies are available to be implemented SMR plants to produce blue hydrogen, including, chemical absorption, membrane technology, adsorption, and cryogenic separation (Voldsgaard et al., 2016). Although all technologies have their benefits and disadvantages. Chemical absorption using amine solvents (e.g., MEA, MDEA, and MDEA/PZ) is widely regarded as the most mature and commercially implemented technology due to its high CO<sub>2</sub>-capturing capacity and selectivity (Yun et al., 2020). Nevertheless, its main disadvantage is its high capital and operational costs. The cost of the absorption process is mainly dependent upon the CO<sub>2</sub> removal efficiency and the solvent regeneration energies (Yun et al., 2021). Therefore, researchers focused on making the absorption process more cost-effective by either investigating the most efficient and less energy-intensive solvents (Khalifa et al., 2022) or by improving the process design to reduce the energy requirements (Nazir et al., 2019).

Numerous studies have reported the implementation of an amine-based CO<sub>2</sub> capture facility in the SMR plant using flue gas, shifted synthesis gas and PSA tail gas streams. Collodi and Wheeler performed an economic analysis to compare the feasibility of CO<sub>2</sub> capture from the flue gas and shifted synthesis gas streams respectively using the MEA and MDEA solvents (Collodi, 2010). Later Roussanly et al. also evaluated the application of the MEA-based CO<sub>2</sub> absorption process to flue gas processing (Roussanly et al., 2020). It has been reported that with the retrofitting CO<sub>2</sub> absorption facility to the SMR plant the cost of hydrogen production increases from 12.1 c€/Nm<sup>3</sup> to 18.1 c€/Nm<sup>3</sup> (Roussanly et al., 2020). Moreover, the cost per unit of hydrogen produced is more in the case of flue gas processing because of the high flow rates and lower total pressures (Collodi, 2010). Similarly, Soltani et al. analyzed

the feasibility of CO<sub>2</sub> absorption using three of the CO<sub>2</sub> capture locations in SMR plants (Soltani et al., 2014). The effect of a steam-to-carbon ratio on the suitability of CO<sub>2</sub> capture locations has been studied and found that the processing of shifted synthesis gas stream is probably the most favorable due to high partial pressures, whilst the flue gas processing option is also improved by the enrichment of oxygen at the lower steam-to-carbon ratios (Soltani et al., 2014).

Most of the studies focused on the processing of the PSA inlet stream using MDEA solvents under high-pressure conditions. For instance, Meerman et al. evaluated the coupling of the CO<sub>2</sub> capture facility to the shifted synthesis gas using the solvents of MDEA and MDEA-PZ blends to achieve 60% of the total plant CO<sub>2</sub> capture (Meerman et al., 2012). It has been reported that the use of imported steam and electricity can reduce CO<sub>2</sub> avoidance costs by 45% and the addition of 5% PZ in MDEA can also reduce the absorber size by 70% thus the capital costs. Similarly, Antonini et al. studied the process optimization for the design of MDEA-based CO<sub>2</sub> capture systems for shifted synthesis gas by applying the multiple objective function optimization over different flowsheet designs (Antonini et al., 2021). Limited studies have been reported for the processing of PSA tail gas using amine solvents because of its high CO<sub>2</sub> contents and low total pressures which make it a less favorable option for CO<sub>2</sub> capture. Nevertheless, Pellegrini et al. studied the CO<sub>2</sub> capture feasibility using the PSA tail gas option by implementing an MDEA solvent (Pellegrini et al., 2020) with which several column configurations have been evaluated and determined the optimal solution.

Based on the literature review it can be inferred that most of the studies have been focused on hydrogen production with about 60% of CO<sub>2</sub> capture instead of a high removal rate. This is mainly due to the high plant capital and operational costs. However, this approach is not appropriate to achieve the goal of net-zero emissions by the mid of century. Therefore, it is inevitable to produce blue hydrogen using the established technology by retrofitting the CO<sub>2</sub> absorption plant to capture close to 100% of the produced CO<sub>2</sub>. For this purpose, systematic investigation is required to identify the cost-effective use of the absorption process when multiple positions are available for CO<sub>2</sub> capture.

As mentioned earlier, to remove a very high percentage of CO<sub>2</sub> produced in the SMR plant, either a flue gas stream is processed using a single high-capacity absorption plant or two separate absorption plants are required to simultaneously remove CO<sub>2</sub> from the flue gas stream along with either the PSA feed gas or the PSA tail gas streams. The simultaneous use of a PSA feed gas stream with flue gas is more suitable in comparison to PSA tail gas because of the high inherent stream pressure. This avoids the requirement of a compressor which is unavoidable in the case of the PSA tail gas (Pellegrini et al., 2020). In general, the simultaneous removal of CO<sub>2</sub> from two streams seems to be expensive due to the implementation of two separate absorption plants but the cost can be compensated by reducing the size of both the flue-gas absorption plant and the PSA plant due to the reduction of gas flow rates. In addition, effort can be further made to improve the design of the CO<sub>2</sub> capture process simultaneously using flue gas and PSA inlet streams to reduce the cost. However, no rigorous process design study with techno-economic analysis is reported either to evaluate the absorption process to simultaneously capture CO<sub>2</sub> from the multiple available streams (flue gas, PSA inlet and PSA tail gas) or to compare the available options in the SMR plant using chemical absorption technology.

In this study, an amine-based chemical absorption process has been applied to capture CO<sub>2</sub> from the SMR-based hydrogen production plant using multiple possible options including the usage of single and dual absorption plants and solvents (MEA and MDEA) as well. Moreover, a novel process design approach based on the arrangements for the simultaneous removal of CO<sub>2</sub> from flue gas and the PSA inlet gas stream is proposed, in which a single solvent (MEA) can be used to treat both the flue gas and PSA gas streams simultaneously. The proposed approach aims to further improve the idea of simultaneous treatment of multiple streams including, flue gas and PSA inlet gas using the amine-based absorption technology. This can be operated in such a way that

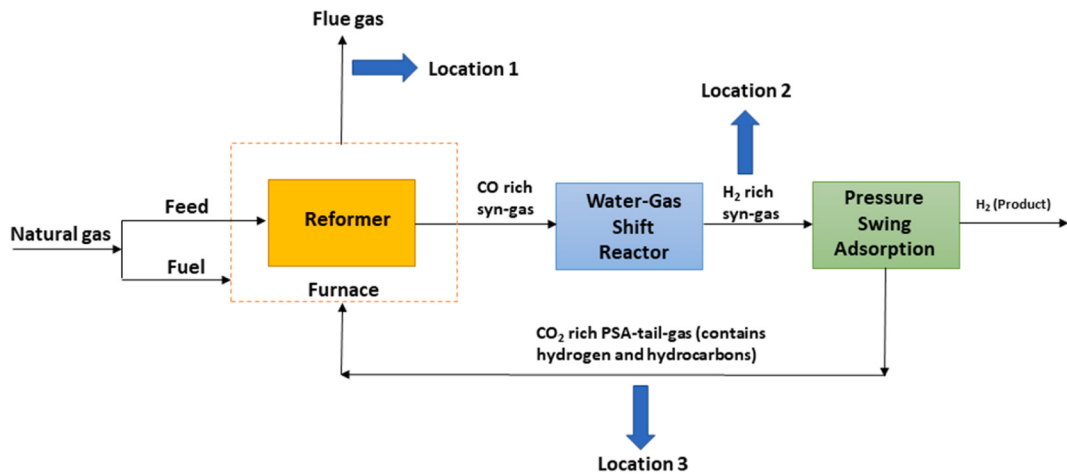


**Fig. 1.** Schematic diagram of SMR process flow.

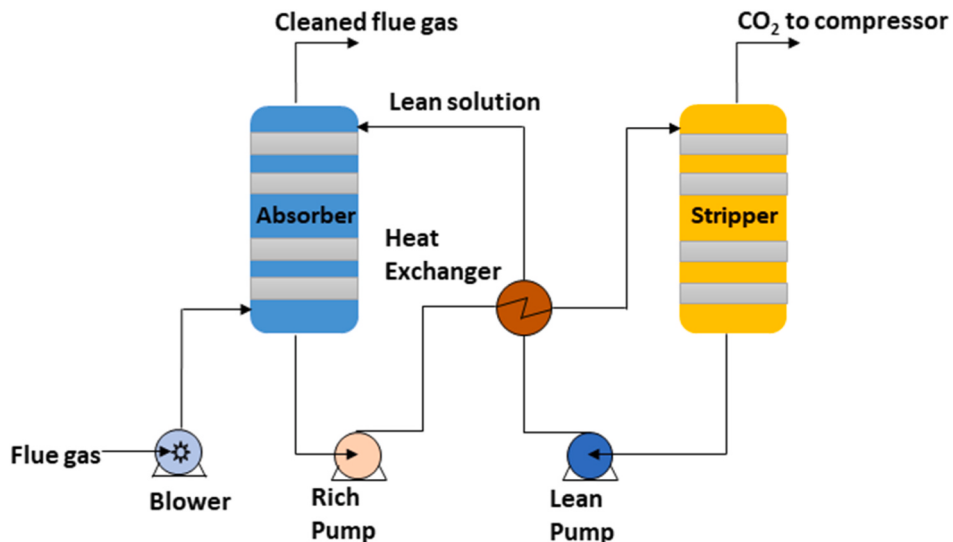


**Fig. 2.** Process flow diagram of standard CO<sub>2</sub> absorption process (Case 1, Cases 4 to 6).

the lean solvent can first remove CO<sub>2</sub> from the flue gas stream at low pressure and later the loaded solvent can further be used to remove CO<sub>2</sub> from the shifted synthesis gas stream over the high-pressure conditions. This single solvent approach has the potential to further reduce the cost by eliminating the need for one stripping column and by reducing the MEA regeneration cost due to the high CO<sub>2</sub> loadings. The high CO<sub>2</sub> loadings of MEA solvent can lead to the reduction of regeneration heat due to the carbamate reversion and hydration reactions (Xu, 2011). The simultaneous capturing of CO<sub>2</sub> at two locations can be proved as a more flexible technology in the long term to handle the high capacity of hydrogen production with CO<sub>2</sub> capture.

For this purpose, the packed column model has been implemented using the rate-based approach implemented in the MATLAB environment to evaluate the effect of absorption process variables, including solvent lean loadings, required solvent flow rates, packing heights, and column diameters on the CO<sub>2</sub> removal efficiencies. Moreover, solvent regeneration heats have been estimated by computing the reaction, vaporization, and sensible heats. Finally, the described cases have been compared for economic evaluation at the conceptual level in terms of the required estimated capital and operational costs of the main equipment.

## 2. Methodology

### 2.1. Base case

In this study, the IEAGHG technical report (IEAGHG) has been considered for the demonstration of the CO<sub>2</sub> capture process from an SMR-based hydrogen production plant. Fig. 1 shows the process diagram of the SMR-based hydrogen production plant. Natural gas enters the reformer as feed and fuel in its furnace. The produced gas is passed to the catalytic shift reactor at high pressures where the most of CO is reacted with steam to increase the yield of hydrogen and reduce CO concentration. Finally, the hydrogen is separated from the shifted synthesis gas using a Pressure Swing Adsorption (PSA) unit. The PSA tail gas is recycled to the furnace of the reformer for heating.

Fig. 1 illustrates three locations available in the SMR plant to capture CO<sub>2</sub>. Location 1 is associated with the flue gas stream which can be used to remove nearly all the produced CO<sub>2</sub>. This stream is available at a total pressure of about 0.02 MPa lower than atmospheric pressure. Location 2 is the PSA inlet stream which is rich in hydrogen and contains about 16% of CO<sub>2</sub>. This stream is available at high total pressures of about 2.6 MPa. Location 3 is the PSA tail gas stream which contains high CO<sub>2</sub> contents around 50% along with some hydrogen and hydrocarbons. This stream

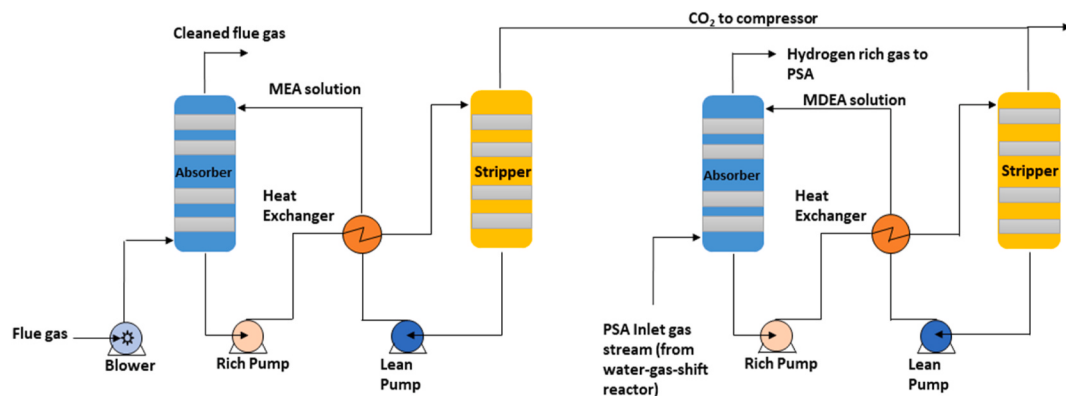


Fig. 3. Process flow diagram of Case 2.

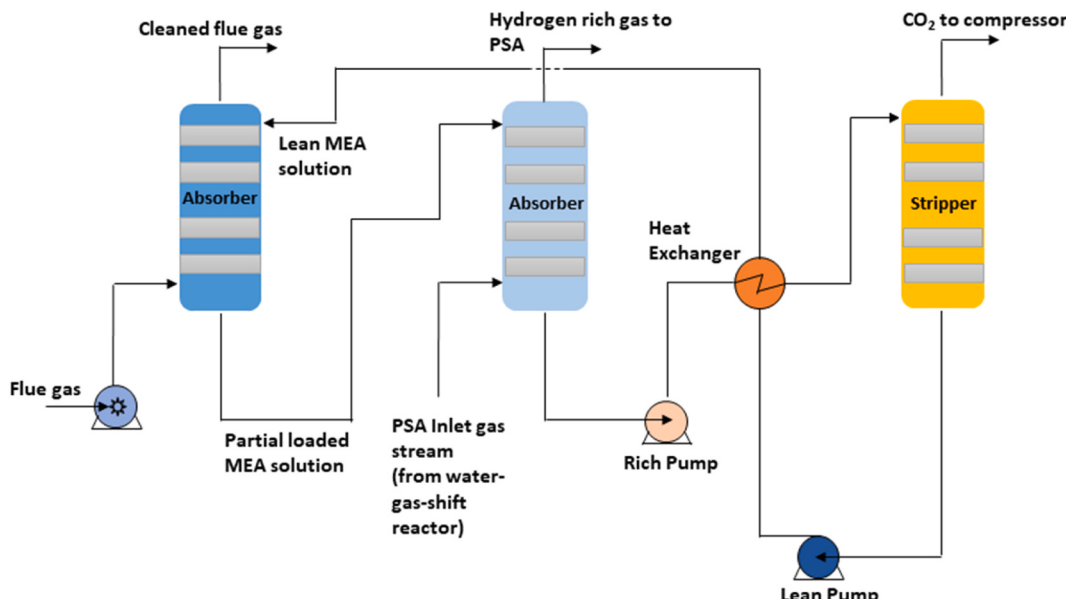


Fig. 4. Process flow diagram of Case 3.

is operated around the atmospheric pressure conditions of about 0.1 MPa.

Six cases have been formulated including, three Cases (1–3) to remove 99% of total plant-produced CO<sub>2</sub>, and three Cases (4–6) to remove about 60% of the total plant-produced CO<sub>2</sub> using the packed absorption column. The column is assumed to be filled with 5 cm stainless steel pall rings.

## 2.2. Cases with high CO<sub>2</sub> removal rate

To remove most of the CO<sub>2</sub> from the plant either only the flue gas stream (location 1) to use for CO<sub>2</sub> capture or simultaneous flue gas stream and PSA inlet (location 2) streams are considered. A process flow diagram for Case 1 is depicted in Fig. 2. The flue gas is treated using a standard absorption process using 30 wt% MEA solvent. A solvent is highly reactive and thus suitable at lower partial pressures. The blower is provided to maintain the required pressure in the absorber. The rich solvent is stripped out to remove CO<sub>2</sub> in the desorber. In Case 2, CO<sub>2</sub> is simultaneously removed using two plant locations (location 1, and location 2) as shown in Fig. 3. Two absorbers are employed where the flue gas and PSA inlet gas streams are respectively treated using 30 wt% MEA and 40 wt% MDEA solvents. The mentioned amine concentrations are adopted because these are commonly reported in the literature (Ellaf et al., 2023).

The loaded solvents are regenerated in the provided separate desorbers. Case 3 is shown in Fig. 4, it contains two absorbers and one desorber. It also collectively removes CO<sub>2</sub> from the flue gas and PSA inlet streams. But unlike in Case 2, only MEA solvent is sequentially used in both absorbers. First, fresh MEA solvent is fed to a flue gas absorber to remove CO<sub>2</sub> and then the loaded solvent is passed to an absorber of the PSA inlet stream where it further removes CO<sub>2</sub> at high-pressure conditions. Finally, a single desorber is employed to regenerate the MEA solvent.

## 2.3. Cases with partial CO<sub>2</sub> removal

In the SMR plant, individually locations 2 and location 3 can be used to remove CO<sub>2</sub>. However, this removal can only result in partial CO<sub>2</sub> removal, say about 60% of the plant. The standard absorption process can be applied for both locations 2 and 3 as depicted in Fig. 1. Three cases are considered including, the CO<sub>2</sub> absorption from the PSA inlet stream using 30 wt% MEA and 40 wt% MDEA solvents regarded as Cases 4 and 5. Case 6 is for the treatment of PSA tail gas using 50 wt% MDEA solvent. The relatively high MDEA concentration is adopted for Case 6 because of the CO<sub>2</sub>-rich feed conditions. In this case, a blower (shown in Fig. 1) is replaced with the compressor because the PSA tail gas stream contains high CO<sub>2</sub> contents, and the total pressure is at the atmospheric

**Table 1**

Equilibrium constants for modified Kent-Eisenberg model.

Equilibrium constants (M) $k_i = a_1/T + a_2 \ln T + a_3$	$a_1$	$a_2$	$a_3$	Temperature range (K)	Source
$k_{1MEA}$	-5851.11	0.0	-3.3636	298–413	Aboudheir et al. (2003)
$k_{1MDEA}$	-8483.95	-13.823	87.39	298–333	Haji-Sulaiman et al. (1998)
$k_2$	-3090.83	0.0	6.69425	298–413	Aboudheir et al. (2003)
$k_3$	-12092.1	-36.78	235.482	273–498	Edwards et al. (1978)
$k_4$	-12431	-35.48	220.067	273–498	Edwards et al. (1978)
$k_5$	-13445.9	-22.47	140.932	273–498	Edwards et al. (1978)

pressure condition. 10–11 bar pressure is reported to be used for the treatment of PSA tail gas (Pellegrini et al., 2020), so 10 bar pressure is adopted for this study.

### 3. Process modelling and simulation of the absorption process

#### 3.1. Rate-based modelling for an absorption column

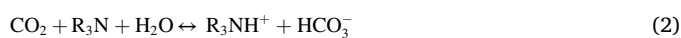
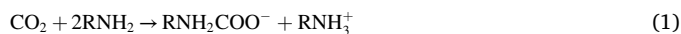
The above-described cases of the  $\text{CO}_2$  absorption process have been simulated using the rate-based model implemented in the MATLAB environment. The model is based on our earlier published studies using MEA (Shahid et al., 2019) and MDEA (Shahid et al., 2021) solvents. The feed gas streams mainly contain  $\text{CO}_2$ , and  $\text{H}_2$  or air with a small number of other components such as CO, methane, and other hydrocarbons. For simplicity in model calculations, the feed gas is assumed as a binary component system using two major components such as  $\text{CO}_2$  and  $\text{H}_2$  in the case of PSA inlet and PSA tail gas streams and  $\text{CO}_2$  and air in the case of flue gas. The main assumptions of the model are described here, and details can be found elsewhere for MEA (Shahid et al., 2019) and MDEA (Shahid et al., 2021) systems.

1. The model is based on the two-film theory and the packed column is segmented into two sections based on the rich  $\text{CO}_2$  loading values ( $\alpha_{Rich}$ ) (section 1:  $\alpha_{Rich} < 0.5$  for MEA and  $\alpha_{Rich} < 1$  for MDEA, section 2:  $\alpha_{Rich} > 0.5$  for MEA and  $\alpha_{Rich} > 1$  for MDEA).
2. In section 1, the reaction lies in the fast reaction regime such that in case of MEA it is completed in a liquid-film while for MDEA it is continued in the bulk of the liquid. In the second section, the reaction is assumed as a slow reaction and mainly completed in the bulk of the liquid.

The main chemical reactions that take place during the absorption process using primary (MEA) and tertiary amines (MDEA) are summarized in Eqs. (1)–(9).

In the case of MEA, the most accepted reaction scheme is the zwitterion mechanism. It is a two-step reaction, in the first step MEA reacts with  $\text{CO}_2$  to form a zwitterion ion which further reacts with another MEA molecule in the second step and carbamate is formed. The overall reaction is shown as Eq. (1). The carbamate formation is limited to 0.5 mol/mol  $\text{CO}_2$  loadings and is a fast and exothermic reaction. However, above 0.5 mol/mol, carbamate reversion takes place as shown in Eq. (4). In addition, the  $\text{CO}_2$  absorption is taking place due to the hydration reactions as explained by reactions Eqs (7)–(9).

In the case of tertiary amines, i.e., MDEA, the reaction mechanism is mostly explained by the base-catalyzed hydration reaction. According to this reaction scheme, the MDEA molecule reacts with a water molecule to generate a  $\text{OH}^-$  ion which converts  $\text{CO}_2$  into bicarbonates and carbonates. In an overall reaction, each MDEA molecule consumes one  $\text{CO}_2$  molecule as shown in Eq. (2). Thereby, above one mol/mol  $\text{CO}_2$  of MDEA, further  $\text{CO}_2$  can only be dissolved by the direct hydration reactions.



The governing equations of the rate-based model are described using Eqs. 10–15. Material and energy balance for the gas and liquid phase are separately implemented using the small differential packing sector  $dz$ .  $y_{\text{CO}_2}$  and  $x_{\text{CO}_2}$  show the  $\text{CO}_2$  mole fraction in the gas phase and liquid phase respectively.  $T_G$  and  $T_L$  are the gas and liquid phase temperatures.  $G$  and  $L$  are the total gas and liquid flow rates.

$$\frac{dy_{\text{co}2}}{dz} = - \frac{N_{\text{co}2}a_e(1 - y_{\text{co}2})}{G} \quad (10)$$

$$\frac{dG}{dz} = - N_{\text{co}2}a_e \quad (11)$$

$$\frac{dx_{\text{co}2}}{dz} = - \frac{N_{\text{co}2}a_e(1 - x_{\text{co}2})}{L} \quad (12)$$

$$\frac{dL}{dz} = - N_{\text{co}2}a_e \quad (13)$$

$$G \frac{dT_G}{dz} = - \frac{h_g a_e (T_G - T_L)}{\sum_i^n c p_i y_i} \quad (14)$$

$$L c p_i \frac{dT_L}{dz} = G \sum_i^n c p_i y_i \frac{dT_G}{dz} + G c p_{\text{co}2} (T_G - T_L) + G (\Delta H_R) \frac{dy_{\text{co}2}}{dz} \quad (15)$$

The gas and liquid phase material and energy balances are formulated using the molar flux over the gas-liquid interface, which is shown in Eqs. (16) and (17), where  $f_{\text{co}2}$  and  $f_{\text{co}2i}$  respectively show the fugacity of  $\text{CO}_2$  in the gas bulk and the gas-liquid interface. Fugacity and total pressure are related using Eq. (18), where  $\phi_{\text{CO}_2}$  is the fugacity coefficient and estimated using Peng-Robinson equation of state (EOS). The interfacial  $\text{CO}_2$  concentration is determined using Eq. (19), where  $E$  is the enhancement factor which defines the effect of chemical reaction on the mass transfer.  $k_g$  and  $k_L$  are mass transfer coefficients for gas and liquid respectively and  $a_e$  is the gas-liquid effective packing area. These parameters are estimated using Onda et al.'s (Onda et al., 1968) and Billet and Schultties (Billet and Schultties, 1993) correlations respectively for the  $\text{CO}_2$ -MEA system considered for model validation and the studied Cases (1–6).  $C_{\text{CO}_2e}$  is the equilibrium concentration of  $\text{CO}_2$  in the liquid bulk phase. In MEA- $\text{CO}_2$  and MDEA- $\text{CO}_2$  absorption systems, enhancement factor (E) can be estimated using Wellek et al.'s (Wellek et al.,

1978) explicit correlation shown in Eq. (20). In case of CO<sub>2</sub>-MEA reaction below 0.5 mol/mol CO<sub>2</sub> loadings, the equilibrium concentration of CO<sub>2</sub> ( $C_{CO2e}$ ) is negligible due to the fast chemical reaction and thus can be ignored in Eq. (19) (Tontiwachwuthikul et al., 1992). However, in the case of the CO<sub>2</sub> loading above 0.5 mol/mol in MEA-CO<sub>2</sub> system, the reaction is slow so  $C_{CO2e}$  calculations are required to estimate interfacial CO<sub>2</sub> concentration using Eq. (19). Similarly, in the case of CO<sub>2</sub>-MDEA system  $C_{CO2e}$  cannot be ignored because the reaction is slow and is not complete in the liquid film. Therefore, for the cases of CO<sub>2</sub>-MEA and CO<sub>2</sub>-MDEA systems equilibrium CO<sub>2</sub> concentration is estimated using the modified Kent-Eisenberg thermodynamic model (Haji-Sulaiman et al., 1998). The related equations for the MEA-CO<sub>2</sub> and MDEA-CO<sub>2</sub> systems are respectively shown as Eqs. (21) and (22), where the CO<sub>2</sub> physical solubility and its partial pressure relationship is described using Henry's Law (Suleman et al., 2015). The hydrogen ion concentration and total amine balance are calculated using amine, CO<sub>2</sub> and electro-neutrality balance, for which more details can be found in the reference (Suleman et al., 2015). The equilibrium constants ( $K_1-K_5$ ) of the reactions shown in Eqs. (3)–(7) for the MEA-CO<sub>2</sub> and MDEA-CO<sub>2</sub> systems are tabulated as Table 1.

$$N_{CO2} = k_g(f_{CO2} - f_{CO2i}) \quad (16)$$

$$N_{CO2} = Ek_L^o(C_{CO2i} - C_{CO2e}) \quad (17)$$

$$f_{CO2i} = y_{CO2} P \emptyset_{CO2} \quad (18)$$

$$f_{CO2i} = \frac{f_{CO2} + \frac{Ek_L^o C_{CO2e}}{k_g}}{1 + \frac{Ek_L^o H}{k_g}} \quad (19)$$

$$E = 1 + \frac{1}{\left[ \left[ \frac{1}{E_\infty - 1} \right]^{1.35} + \left[ \frac{1}{E_1 - 1} \right]^{1.35} \right]^{\frac{1}{1.35}}} \quad (20)$$

$$\alpha = \frac{\left[ [CO_2] + \frac{K_3 [CO_2]}{[H^+]} + \frac{K_3 K_4 [CO_2]}{[H^+]^2} + \frac{K_3^m K_3 [CO_2]}{K_2 [H^+]^2} \left[ \frac{2K_3 K_4 [CO_2] + K_3 [CO_2] [H^+] + K_5 [H^+]^3}{[H^+]^2 - \frac{K_3^m K_3 [CO_2]}{K_2}} \right] \right]}{[Alk_{total}]} \quad (21)$$

$$\alpha = \frac{\left[ [CO_2] + \frac{-K_3 [CO_2]}{[H^+]} + \frac{K_3 K_4 [CO_2]}{[H^+]^2} \right]}{[Alk_{total}]} \quad (22)$$

### 3.2. Calculation of the regeneration heat of solvent

The regeneration heat of the solution is generally determined by the modelling of the desorber. However, it can also be estimated using the simple theoretical approach without a complete designing of the desorber. The total heat required to regenerate MEA or MDEA solvent is equal to the sum of the sensible heat, the reaction heat and the stripping heat as shown in Eq. 23 (Song et al., 2008). Sensible heat depends upon the required temperature duty or the difference between the top and bottom temperature of the desorber and the solvent flowrates. Q<sub>R</sub> is equal to heat of reaction which can simply be estimated using the empirical correlations of heat of reaction of CO<sub>2</sub>-MEA and MDEA. In this study, the correlation for CO<sub>2</sub>-MEA system is adopted which is valid over the high CO<sub>2</sub> loading range (Xu, 2011). Q<sub>V</sub> is the stripping heat which is the most important factor in regeneration heat calculations that controls the profile of regeneration energy along the striping column. It depends upon the equilibrium pressure of water vapors and the CO<sub>2</sub> at the bottom and top of the striping column. In literature, it has been estimated using

the product of water heat of vaporization and the ratio of equilibrium pressure of water vapors to CO<sub>2</sub> only at the top of the desorber (Nwaoha et al., 2017). However, the effect of the ratio of water vapors to CO<sub>2</sub> equilibrium pressure is the most dominant at the bottom of the desorber, where the relative pressure of CO<sub>2</sub> is quite low in comparison to the water vapors which results in high regeneration heat. Therefore, in this study, this equation includes the log-mean pressure difference for both water and CO<sub>2</sub> over the top and bottom conditions of the desorber shown as Eq. (26). The temperature for the inlet and outlet of the desorber are assumed to be respectively fixed as 105 °C and 125 °C for MEA solvent systems and 100 °C and 115 °C for MDEA systems for all the studied Cases (1–6). The water vapor pressure is estimated using the Antonie equation (P<sub>H2OBOTTOM</sub> and P<sub>H2OTOP</sub>). The CO<sub>2</sub> equilibrium pressure for CO<sub>2</sub> rich MEA conditions (P<sub>CO2TOP</sub>) is estimated using the semi-empirical equilibrium model of Suleman et al. (2021), whereas P<sub>CO2TOP</sub> and P<sub>CO2BOTTOM</sub> for MDEA solvent and P<sub>CO2BOTTOM</sub> for MEA solvent are estimated using the equilibrium model proposed by Posey et al. (1996). These models are selected for the solvent regeneration heat calculations instead of the modified Kent-Eisenberg model that has been used in the absorber calculations because of their higher accuracy at the desorber conditions.

$$Q_{Solvent-regeneration} = Q_S + Q_R + Q_V \quad (23)$$

$$Q_S = \frac{V \rho C_p \Delta T}{(\alpha_{Rich} - \alpha_{Lean})n} \quad (24)$$

$$Q_R = \Delta H_R \quad (25)$$

$$Q_V = \Delta H_V \frac{\frac{(P_{H2OBOTTOM} - P_{H2OTOP})}{log \left( \frac{P_{H2OBOTTOM}}{P_{H2OTOP}} \right)}}{\frac{(P_{CO2TOP} - P_{CO2BOTTOM})}{log \left( \frac{P_{CO2TOP}}{P_{CO2BOTTOM}} \right)}} \quad (26)$$

### 4. Techno-economic analysis

The economic analysis of the earlier described different CO<sub>2</sub> capture process cases for a SMR-based hydrogen production plant has been performed at conceptual level with the evaluation of major elements for capital and operating cost. The capital cost is determined in terms of the purchase cost of absorber, and desorber columns, lean and rich solvent pumps, blower and compressor, and lean-rich solvent heat exchanger. The operating cost is evaluated in terms of the electricity requirement for pumps, blower and compressor and steam requirements for the solvent regeneration in desorber. Finally, to compare the studied systems the annualized cost (A<sub>NC</sub>) is estimated using the total estimated purchase costs and the annual operating costs as shown in Eq. (27).

$$A_{NC} = C_{OP} + 0.2 \sum_i^n C_{P-i} \quad (27)$$

Where, C<sub>OP</sub> is the total annual operating cost and C<sub>P-i</sub> is the purchase cost of an equipment i, which includes, absorber, desorber, heat exchanger, pumps, blower and compressor. The details of the purchase and operating cost estimation will come in the later section.

The correlations for the estimation of purchase cost have been taken from the reference (Seider et al., 2009), which has reported the purchase cost parameters based on the chemical engineering cost index (CECI) of 500 for year 2006. In this study, the purchase costs are reported according to the CECI of 699.97 2021 (Junsittiwate et al., 2022).

#### 4.1. Capital cost of absorbers, desorbers, and heat exchangers

The purchase cost of absorber is estimated using Eq. (28), where C<sub>P-Vessel</sub> is the purchase cost of empty vessel including, nozzles, manholes and supports based on weight calculations as shown in Eq. (28) with the

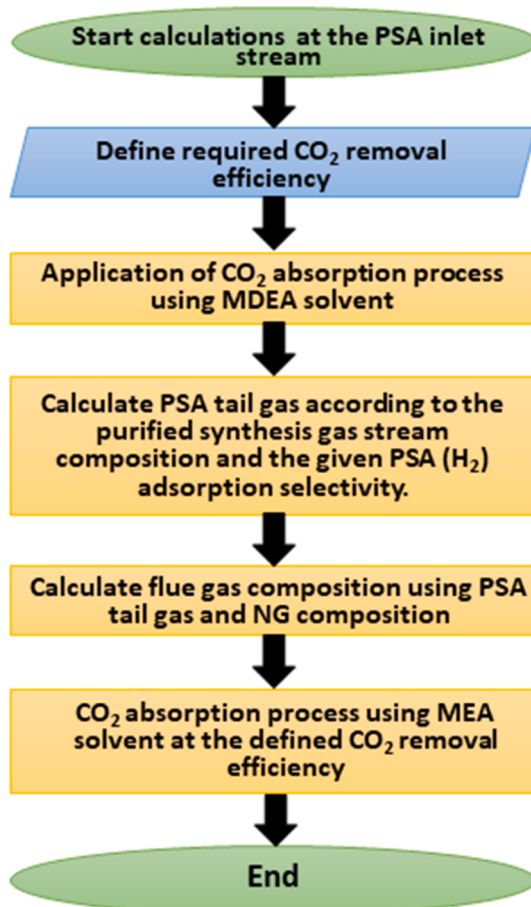


**Fig. 5.** Computational procedure for the CO<sub>2</sub> absorption process from PSA stream.

application range of 9,000–25,000,000 lbs.  $F_M$  is the factor for materials of construction and for carbon steel and stainless steel 304, its values respectively are 1.0 and 1.7.

$$C_{P-Absorber} = F_M C_{P-Vessel} + C_{P-PL} + V_{Pack} C_{P-Pack} + C_{P-DR} \quad (28)$$

$$C_{P-Vessel} = \exp\{7.2756 + 0.18255[\ln(W)] + 0.02297[\ln(W)]^2\} \quad (29)$$

$C_{P-Pack}$  is the installed cost of the packing in USD per cubic feet. The installed cost for the 2-inch stainless Raschig rings is given as USD 110/ft<sup>3</sup> (Seider et al., 2009).  $C_{P-DR}$  is the installed cost of high-performance liquid distributors required for the reliable performance of packing. It can be estimated as USD 125/ft<sup>2</sup> of column cross-sectional area.  $C_{P-PL}$  is the added cost that defines platforms and ladders as a function of column diameter,  $D_{Absorber}$ , in feet, and tangent-to-tangent length of the shell (total column height),  $L$  in feet shown by Eq. (30). The weight of column vessel ( $W$ ) is estimated using Eq. (31), where  $t_S$  and  $\rho_M$  respectively are the column wall thickness (inches) and material density (lbs/ft<sup>3</sup>). In the case of higher pressure inside the column than the external pressure, the effect of pressure on the column thickness can be estimated using Eqs. (32) and (33).  $P_d$  is the internal design gauge pressure,  $S$  is the maximum allowable stress (lbf/in<sup>2</sup>) at the designed temperature and  $E_w$  is the fractional welding efficiency.

$$C_{P-PL} = 300.9(D_{Absorber})^{0.63316}(L_{Absorber})^{0.80161} \quad (30)$$

$$W = \pi(D_{Absorber} + t_s)(L_{Absorber} + 0.8D_{Absorber})t_s\rho_M \quad (31)$$

$$t_p = \frac{P_d D_{Absorber}}{2SE_w - 1.2P_d} \quad (32)$$

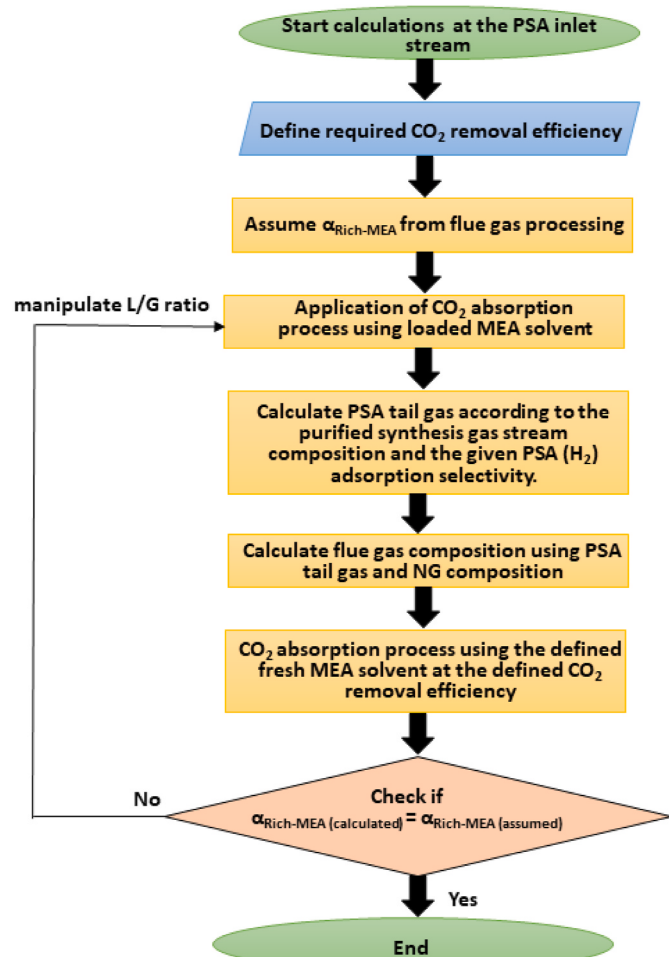


**Fig. 6.** Computational procedure for CO<sub>2</sub> absorption process from flue gas and PSA stream.

$$P_d = \exp\{0.60608 + 0.9165[\ln(P_o)] + 0.0015655[\ln(P_o)]^2\} \quad (33)$$

For simplicity, the purchase cost of the desorber columns and the heat exchanger are estimated using the ratio of absorber unit price to the desorber and heat exchanger using the purchase cost data reported by (Ali et al., 2019) and (Aromada et al., 2020). The relevant Eqs. are given as (34)–(35a).

$$C_{P-desorber} = 0.28C_{P-Absorber} \quad (34)$$

$$C_{P-HX} = 0.15C_{P-Absorber} \quad (35a)$$

#### 4.2. Capital cost of rich and lean solvent pumps

The total purchase cost of the pump is estimated using the cost of the pump and driving motor as shown in Eq. (38).  $C_{B,j}$  (where  $j$  = pump or motor) stands for the purchase cost that is estimated for both the pump and driving motor using the correlations in Eqs. (39) and (40). For the pump, it is a function of the size factor which is defined in terms of the required flowrates and the total head as given in Eq. (41), whereas the motor cost is the function of required power which is estimated using the efficiency relations as shown in Eqs. (42, 43 and 44). In this study, the lean pump cost is estimated using the simulated conditions. However, for the rich amine pump, the cost is estimated using the ratio of lean pump cost to rich pump cost taken from the literature (Ali et al., 2019) as shown in Eq. 38. For  $S$  in the range of 400–10000, where  $S$  is the size factor and given as in Eq. (41) and  $Q$  is the flow rate in gallons per

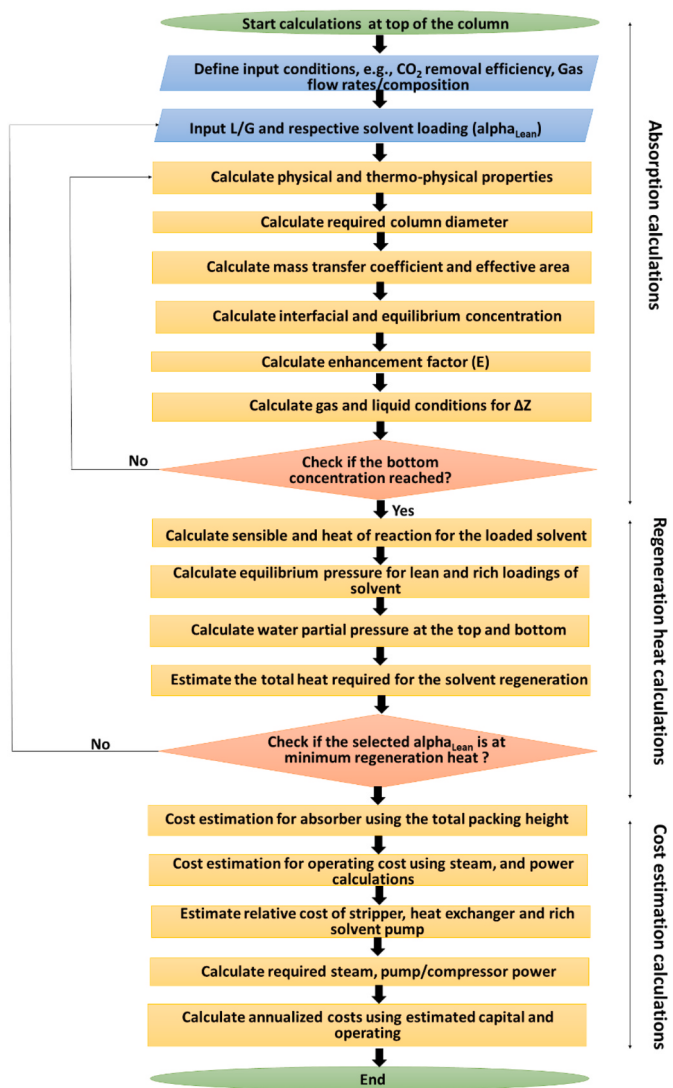


Fig. 7. Computational algorithm of model.

minute and  $H$  is the pump head in feet of the fluid.

$$C_{P-pump} = F_{TP} F_M C_{B-pump} \quad (35b)$$

$$C_{P-pump-motor} = F_{TM} C_{B-pump-motor} \quad (36)$$

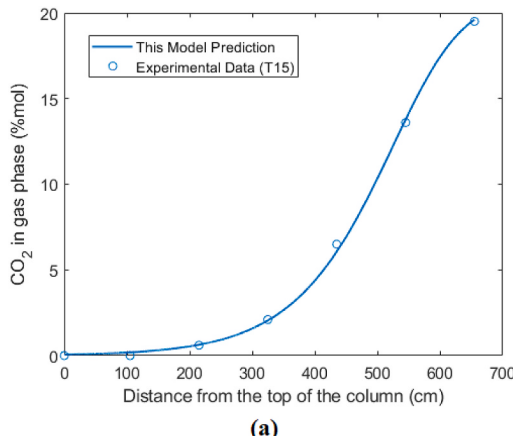


Fig. 8. Validation of the rate-based model.

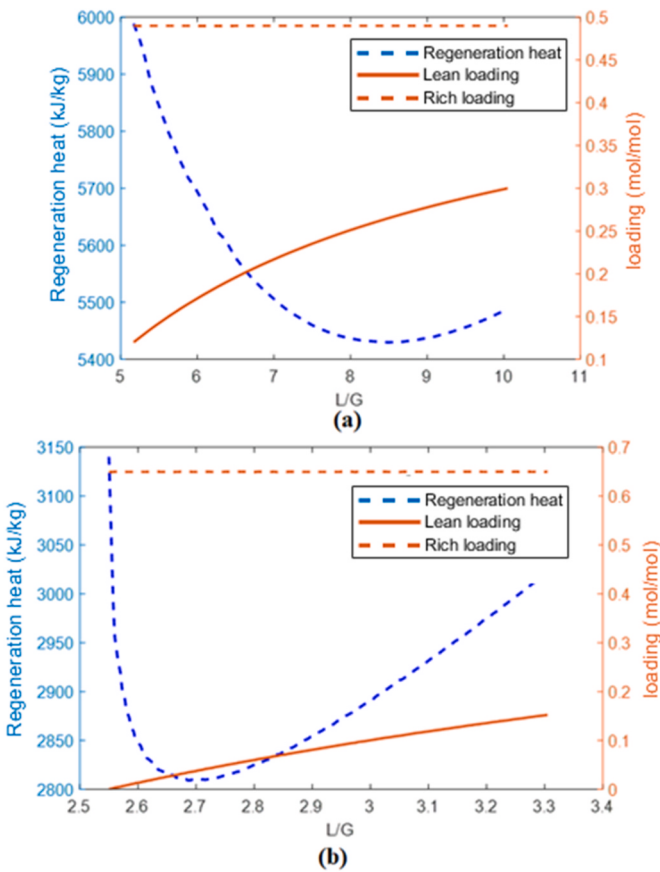


Fig. 9. (a) Case 1 (MEA system), L/G and lean loading selection, (b) Case 4 (MDEA system), L/G and lean loading selection.

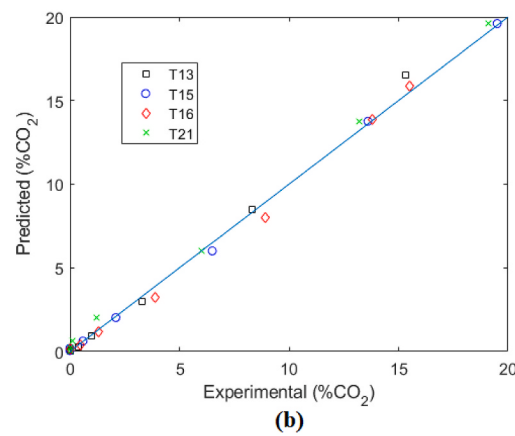
$$C_{P-PumpL} = C_{P-pump} + C_{P-pump-motor} \quad (37)$$

$$C_{P-PumpR} = 0.8485 C_{P-pumpL} \quad (38)$$

$$C_{B-pump} = \exp\{9.7171 + 0.6019[\ln(S)] + 0.0519[\ln(S)]^2\} \quad (39)$$

$$C_{B-pump-motor} = \exp\{5.8259 + 0.13141[\ln(P_C)] + 0.053255[\ln(P_C)]^2 + 0.028628[\ln(P_C)]^3 - 0.0035549[\ln(P_C)]^4\} \quad (40)$$

$$S = QH^{0.5} \quad (41)$$



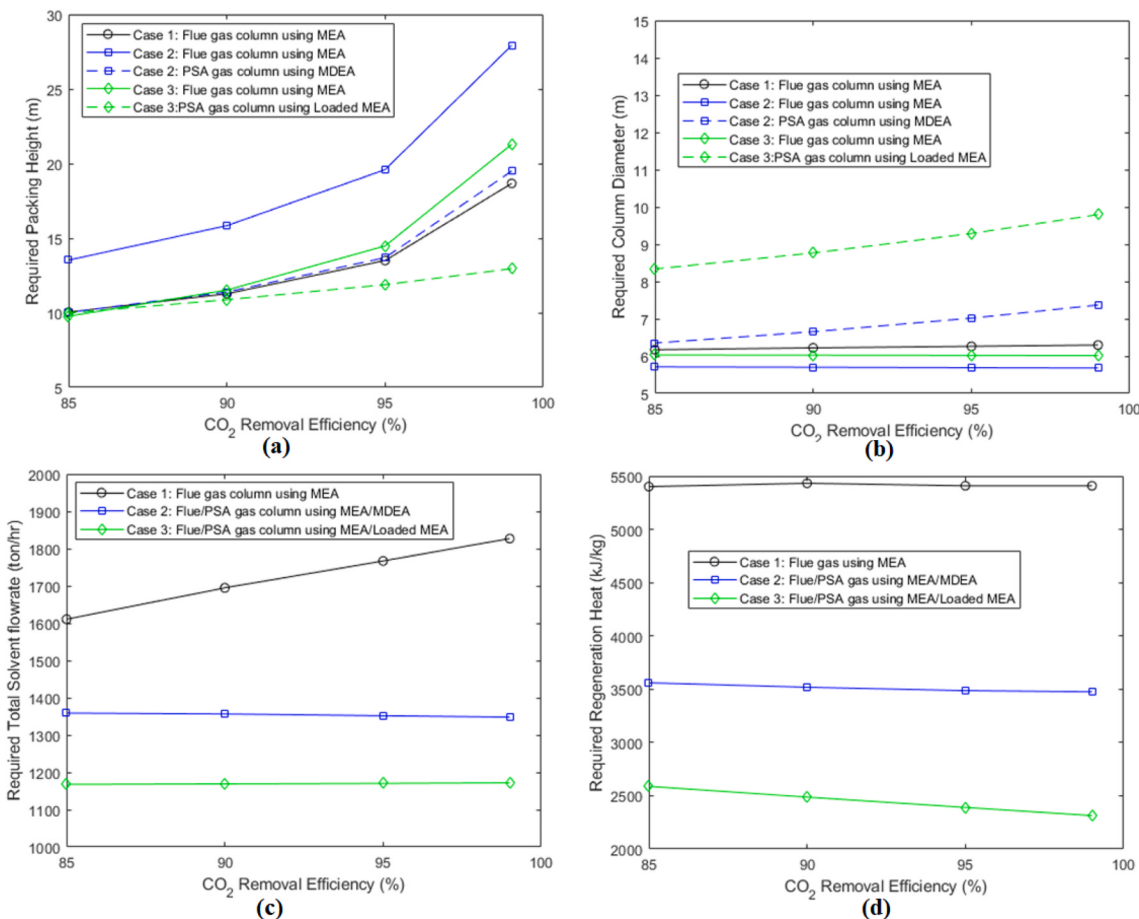
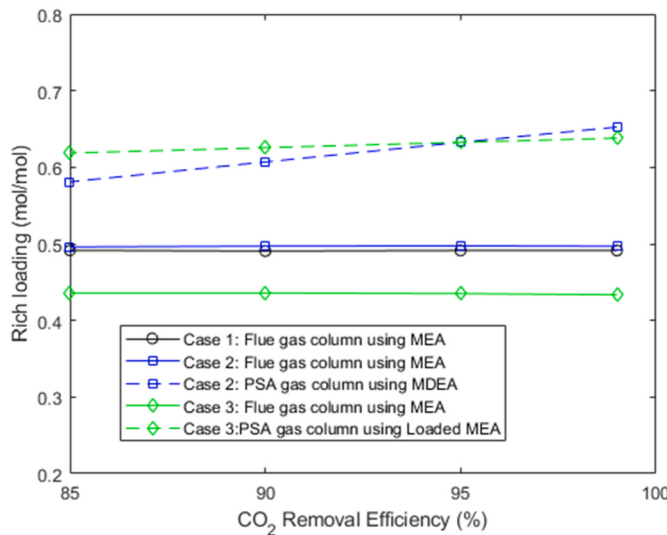


Fig. 10. Design parameters effect for Cases 1 to 3.

Fig. 11. CO<sub>2</sub> loading profiles for Cases 1 to 3.

$$P_C = \frac{P_B}{\eta_M} = \frac{QH\rho}{33000\eta_P\eta_M} \quad (42)$$

$$\eta_P = -0.316 + 0.2015(\ln Q) - 0.01199(\ln Q)^2 \quad (43)$$

$$\eta_M = 0.80 + 0.0319(\ln P_B) - 0.00182(\ln P_B)^2 \quad (44)$$

#### 4.3. Capital cost of blower and compressor

The blower is provided in the cases with flue gas processing whereas the compressor is only used in the case of PSA tail gas treatment. The cost of the blower is estimated using the correlation given in Eq. (45) as a function of consumed power. The power is determined using Eqs. (46) and (47).  $P_B$  is a function of required flowrates, inlet and outlet pressure difference, and  $k$  is assumed as the constant specific heat ratio of 1.4.

$$C_{B-Blower} = \exp\{6.8929 + 0.7900[\ln(P_C)]\} \quad (45)$$

$$P_C = \frac{P_B}{\eta_M} \quad (46)$$

$$P_B = 0.00436 \left( \frac{k}{k-1} \right) \frac{Q_I P_I}{\eta_B} \left[ \left( \frac{P_o}{P_I} \right)^{\frac{k-1}{k}} - 1 \right] \quad (47)$$

Similar to the blower, the compressor purchase cost is determined using Eqs. (48) and (49), where the power is determined using the similar Eqs. of the blower (46 and 47).

$$C_P = F_D F_M C_B \quad (48)$$

$$C_{B-Compressor} = \exp\{7.966 + 0.8[\ln(P_C)]\} \quad (49)$$

#### 4.3.1. Evaluation of operating cost

The annual operating cost is reported in terms of the required steam cost for the solvent regeneration, and the electricity costs of the pumps, compressor, and blower. The cost of steam is assumed as USD 10.5/1000 kg, where steam pressure is 150 psig and the reboiler heat losses

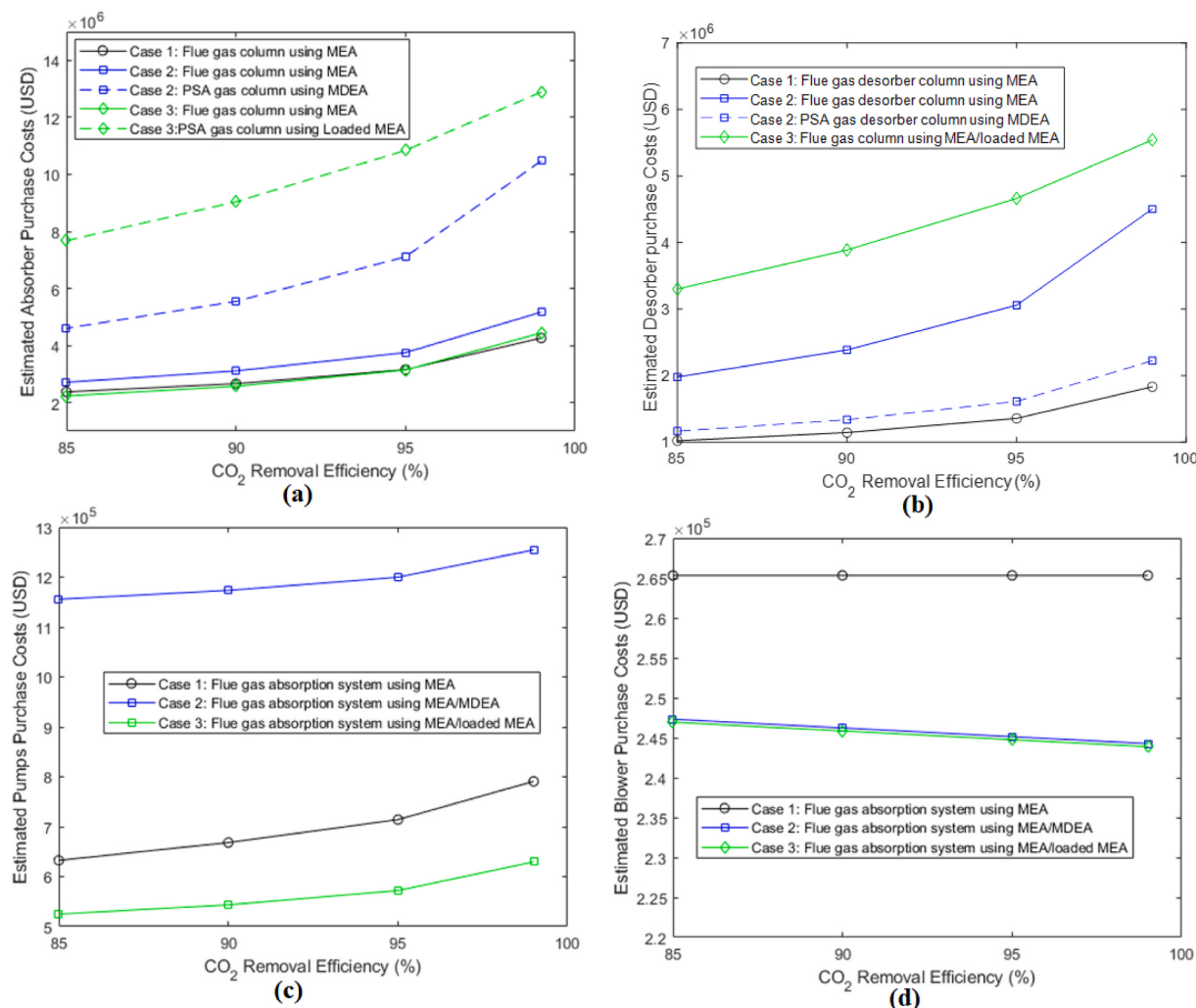


**Fig. 12.** Purchase costs of the main equipment in Cases 1 to 3.

are assumed as 10%. The electricity cost used in the operating cost estimation is assumed as USD 0.07/kWh. The annual plant operation factor is considered as 0.9 for the operating cost estimation in all the used operations.

#### 4.3.2. Key-cost indicators

In the technoeconomic analysis usually the sensitivity of process economy is evaluated by varying the cost of various operating parameters such as fuel, electricity, and steam. In this study the sensitivity of estimated 5- years annualized cost is evaluated as a function of unit electricity and steam costs to compare all the studied Cases 1–6 respectively in the range of USD 0.06–0.18/kWh and USD 8–20/t steam.

## 5. Computational procedure

The feed gas stream for the CO<sub>2</sub> removal process in each of the described or formulated Cases (1–6) is taken according to the material balance given in the referred IEAGHG technical report (IEAGHG, 2017). The stream specifications are tabulated and shown as Tables S1–S3 in the supplementary information. In Cases 1, 4 and 5 of flue gas, PSA inlet and PSA tail gas streams processing the feed gas compositions are as it is considered for the calculations. However, in the case of simultaneous CO<sub>2</sub> removal for Cases 2 and 3, the rebalancing calculations of material and energy balance are required due to the implementation of CO<sub>2</sub> capture for PSA inlet stream. For Case 2 in which CO<sub>2</sub> removal is simultaneously made from the reformer flue gas and PSA inlet stream

using MEA and MDEA solvents respectively, the material balance calculations are carried out with the computational procedure given in Fig. 5. In the first step, CO<sub>2</sub> is removed from the PSA inlet stream and then according to the CO<sub>2</sub> removal efficiency and PSA H<sub>2</sub> separation efficiency (IEAGHG), the PSA tail gas stream is determined. Further, the flue gas composition is also calculated based on the updated PSA tail gas and the natural gas fuel.

In Case 3, CO<sub>2</sub> is removed using the MEA solvent from both the PSA inlet stream and the reformer flue gas stream in such a way that the fresh MEA solvent ( $\alpha_{\text{Lean-MEA}}$ ) first removes CO<sub>2</sub> from the flue gas and then the partially loaded MEA solvent ( $\alpha_{\text{Rich-MEA}}$ ) removes CO<sub>2</sub> from the PSA inlet gas stream. The computational procedure is illustrated in Fig. 6. In calculations, the CO<sub>2</sub> absorption process is first implemented to the PSA inlet gas stream, where the CO<sub>2</sub> loading of the inlet loaded MEA solvent ( $\alpha_{\text{Rich-MEA}}$ ) is unknown at this stage, so it is assumed and shown as  $\alpha_{\text{Rich-MEA}}$  (assumed) in Fig. 6. The material and energy rebalancing of PSA tail gas stream and the reformer flue gas are accordingly calculated. In the subsequent step, the CO<sub>2</sub> removal calculations are performed at the reformer flue gas stream and compared the calculated CO<sub>2</sub> loading of the partially loaded MEA solvent ( $\alpha_{\text{Rich-MEA}} \text{ (calculated)}$ ) with the already assumed MEA loading ( $\alpha_{\text{Rich-MEA}} \text{ (assumed)}$ ) and iteratively manipulating the L/G value until the difference of calculated and assumed CO<sub>2</sub> loading value reaches around zero.

The overall flow of calculations required for the evaluation of formulated cases of the CO<sub>2</sub> absorption process are illustrated in Fig. 7. The calculations can be viewed in three stages, including, the

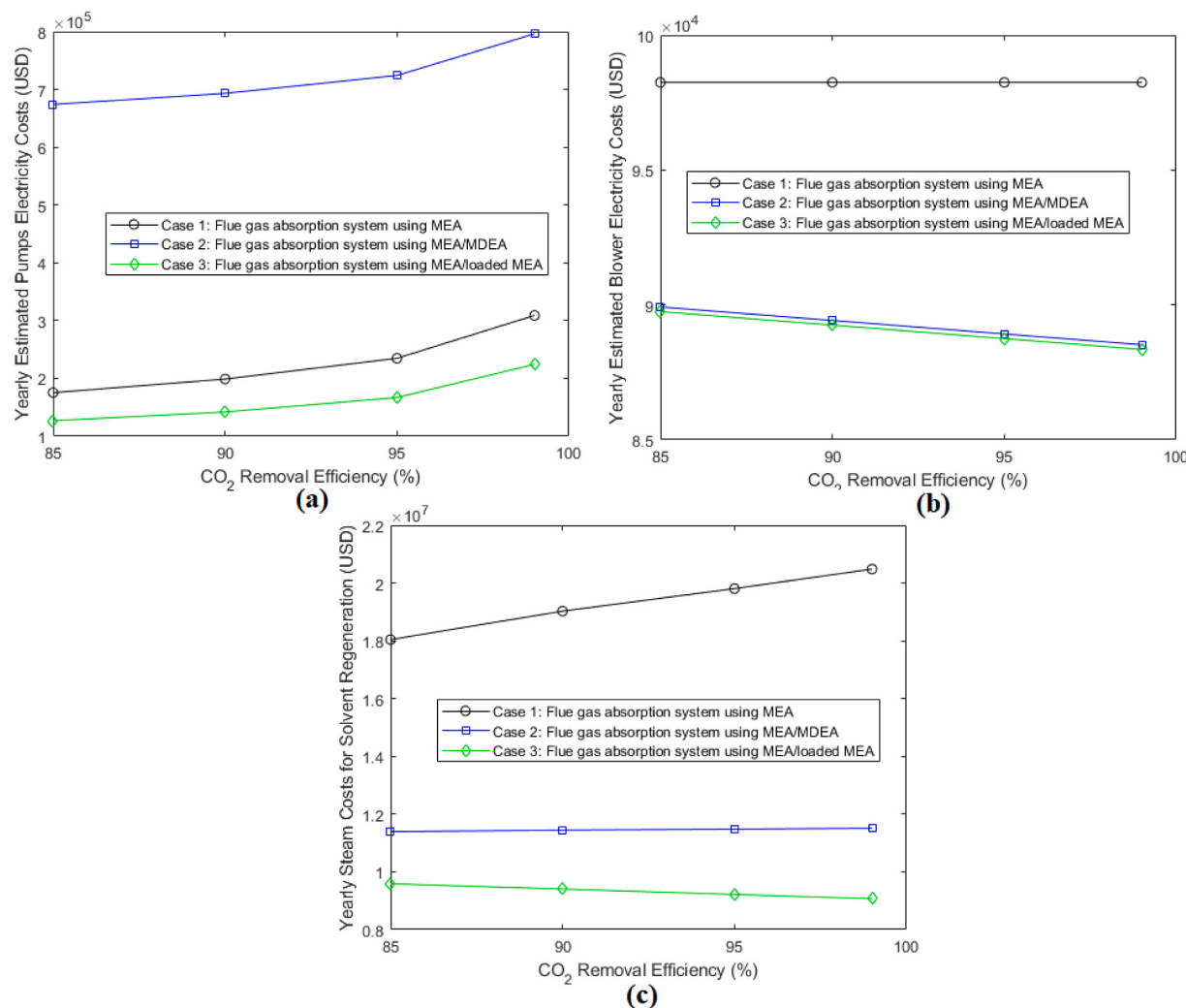


Fig. 13. Operating costs for cases 1-3.

calculations of the absorber, solvent regeneration heat and finally the process cost estimation. For the absorber calculations, the rate-based model described earlier is implemented in a MATLAB environment. The differential equations for the computation of packing height required for the relative CO<sub>2</sub> removal efficiency have been solved using the shooting method. The calculations started at the top of the absorber column, where the conditions of solvent are known or defined but gas conditions are assumed according to the required CO<sub>2</sub> removal efficiency. Initially, the physical, and thermo-physical properties of the gas and solvent are calculated and then enhancement factor and thermodynamic calculations are performed to compute the gas composition for the absorber height sector ΔZ. The calculations are continued until the bottom known gas composition is achieved and the total Z gives the required packing height. In the last step the economic analysis is performed using correlations and methods defined earlier with the simulated parameters (e.g., packing height, column diameter, required solvent flowrates and the regeneration heat duties). The total column height used in the purchase cost estimation is assumed to be two times of the packing height to include the space for packing units, distributors, etc.

## 6. Results and discussion

In this section, firstly the presentation of the used rate-based model is provided. Later the performance comparison of Cases (1–6) for CO<sub>2</sub> capture from a SMR-based hydrogen production plant is described. The

technoeconomic performance of the cases has been evaluated in terms of the process design, including packing height, column diameter, required solvent flowrates and solvent regeneration heat and economics in terms of main equipment purchase and operating cost. The details of the estimated cost parameters are tabulated in the supplementary information as Tables S5–S6.

### 6.1. Validation of the presented rate-based model

The rate-based model described earlier in section 3 has been previously validated using the pilot plant experimental data over a wide range of operating conditions for the CO<sub>2</sub> removal from; flue gas using MEA solvent (Shahid et al., 2020), natural gas using MEA solvent (Shahid et al., 2019), and natural gas using MDEA solvent (Shahid et al., 2021). Nevertheless, in this study a few of the experimental runs (T13, T15, T16 and T21) of CO<sub>2</sub> absorption from flue gas streams have been taken from the literature (Tontiwachwuthikul et al., 1992) for the demonstration of model validation.

Fig. 8 (a) and (b) show the comparison of model predicted and experimental data of CO<sub>2</sub> concentration along the height of the column. Fig. 8 (a) shows excellent agreement between the model predicted curve and the experimental data points of CO<sub>2</sub> concentration along the packing height of the column for the experimental run T15. Besides, multiple runs (T13, T15, T16 and T21) have been tested with the model and parity plot is presented in Fig. 8 (b). It shows excellent correlation between predicted and experimental data points. The coefficient of

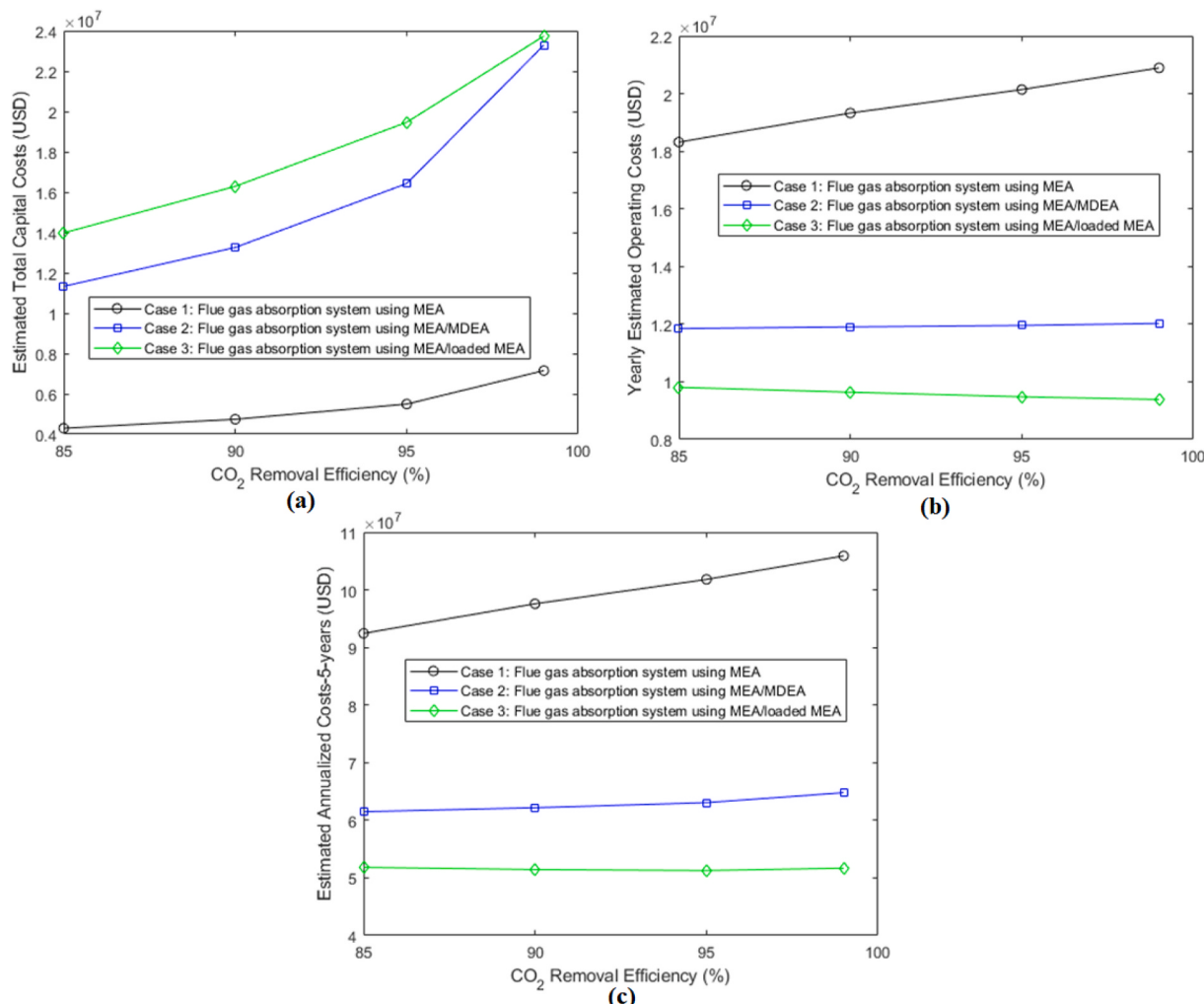


**Fig. 14.** Comparison for total capital, operating and annualized costs for Cases 1 to 3.

correlation (R<sup>2</sup>) is estimated to as 0.99.

#### 6.2. Selection of suitable lean loadings and L/G ratio

The economy of the CO<sub>2</sub> absorption process is largely dependent upon the employed L/G (liquid to gas ratio) and the CO<sub>2</sub> loading ( $\alpha$ ) of a solvent. Fig. 9 (a) shows the variation of regeneration heat required to strip-out CO<sub>2</sub> from the rich solvent as a function of the L/G ratio for the studied Case 1 (Flue gas system with 99% CO<sub>2</sub> removal efficiency). The profiles of CO<sub>2</sub> loading of the lean solvent and the rich solvent are also shown. The lean loading of the solvent is varied from 0.11 to 0.3 mol/mol, whereas the rich loading of the solvent is kept constant at around 0.5 mol/mol. It can be observed that regeneration heat is the highest at the low values of lean loadings and eventually decreases as the solvent lean loading increases and reaches the minimum value of around 0.24 mol/mol. This is because initially at the lower CO<sub>2</sub> loadings, the heat of vaporization is very high. Further, it can be noted that above 0.27 mol/mol of loadings, the regeneration heat again starts to rise. This is because as the L/G ratio further increases, the sensible heat starts to increase due to the high solvent flowrates. The suitable lean loading and L/G for an absorption process can be decided based on the minimum possible regeneration heat. In the presented case, the minimum regeneration heat is found to be around 0.24 mol/mol loadings. Similar to Case 1, 0.24 mol/mol lean loading value is obtained for other MEA solvent-based cases including Case 2 and 3. However, in Case 5, lean loading is determined as 0.19 mol/mol suitable for achieving the minimum

regeneration energy. In literature commonly for the MEA systems, the reported optimal lean solvent loading is around the range of 0.2–0.25 mol/mol (Vega et al., 2020). Similarly, in the case of MDEA solvent systems (Cases 3, 4 and 6), the appropriate lean CO<sub>2</sub> loading is found to be around 0.05 mol/mol for all these cases. The determined appropriate lean loading of MDEA systems lies in the optimal lean loading range (0.05–0.15) as reported in the literature (Pellegrini et al., 2020). The profile of lean CO<sub>2</sub> loading with L/G values for Case 4 is depicted in Fig. 9 (b).

#### 6.3. Results of cases with full CO<sub>2</sub> removal (Cases 1 to 3)

Fig. 10(a–d) shows the effect of CO<sub>2</sub> removal efficiency in the range of 85%–99% on the main process design parameters including packing height, column diameter, required solvent flow rates and solvent regeneration heat for Cases 1 to 3. It can be observed that the required packing height is increased with an increase of CO<sub>2</sub> removal efficiency. In Case 2, for the PSA gas system, it is observed to be maximum among all the presented cases due to the slow kinetics of the CO<sub>2</sub>-MDEA system. The lowest packing height is required in Case 3, where the loaded MEA is used to absorb CO<sub>2</sub>. This is because MEA solvent quickly removes CO<sub>2</sub> over elevated pressure conditions (Tan et al., 2015).

In Fig. 10 (b), the column diameter seems to be nearly constant for most of the cases. However, for Cases 2 and 3 of PSA gas systems, it slightly increases with the CO<sub>2</sub> removal efficiency. This is because of the variation in gas density due to CO<sub>2</sub> removal which is relatively more

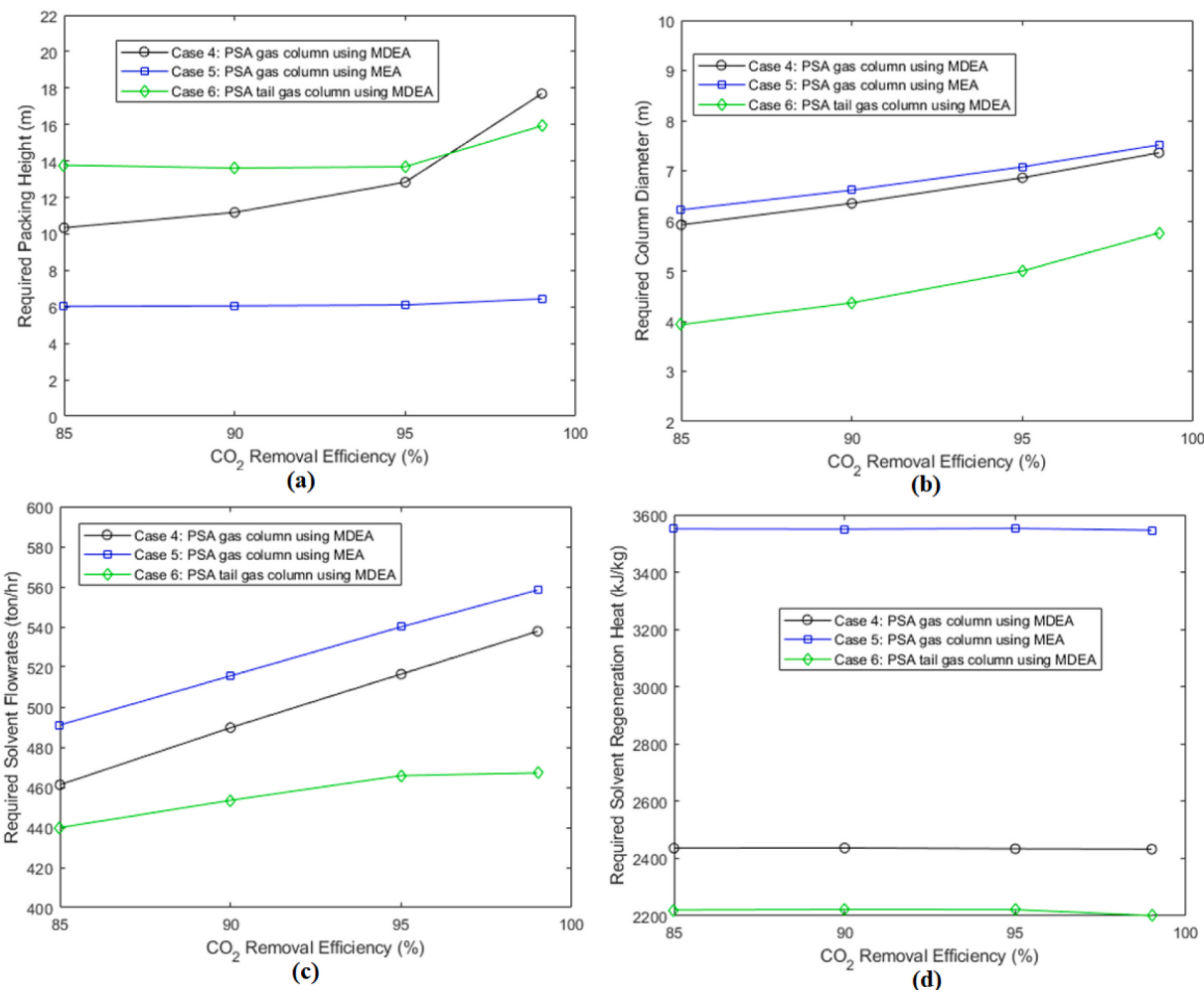


Fig. 15. Design parameters effect for Cases 4 to 6.

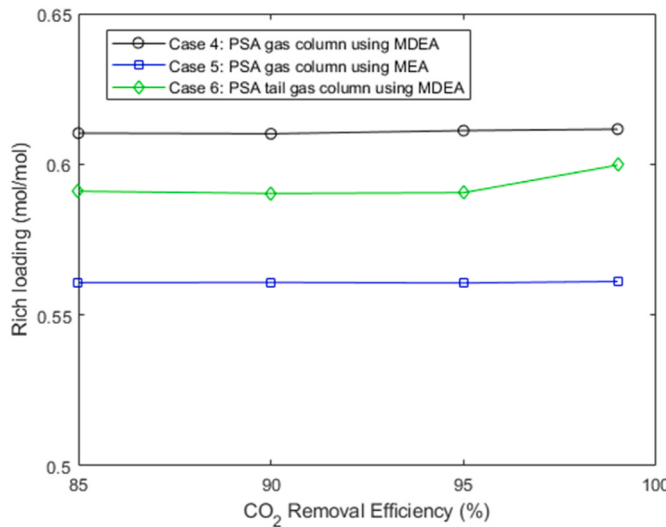


Fig. 16. Rich solvent loadings Cases 4 to 6.

dominant in the case of PSA gas streams in comparison to flue gas systems owing to the presence of lighter gas components, mainly hydrogen in high concentrations. The required solvent flow rate profiles are depicted in Fig. 10 (c). It can be observed that in Case 1, the requirement

of solvent flow rate increases with the increase of CO<sub>2</sub> removal efficiency. This is due to the saturation of MEA solvent at the lower pressure conditions (reaching 0.5 mol/mol loadings). Case 2 solvent profile shows the total MEA and MDEA solvent utilized. Similar profiles of the total MEA consumption in both the flue and PSA gas columns are observed for Case 3. For the profiles of Cases 2 and 3, the required solvent flow rates seem to be nearly constant. This is because in the case of the PSA systems the CO<sub>2</sub> loading is also increased as shown in Fig. 11 which compensates for the requirements of additional solvent flow rates for higher CO<sub>2</sub> removal efficiencies. Nevertheless, the CO<sub>2</sub> loadings for the flue gas systems are constant near 0.5 mol/mol due to the limitation of lower CO<sub>2</sub> partial pressures.

Fig. 10 (d) illustrates the required total solvent regeneration heat profiles for Cases 1 to 3. It seems that the effect of CO<sub>2</sub> removal efficiency is negligible in Case 1, whereas in Cases 2 and 3 it slightly reduces the regeneration heat with the increase of CO<sub>2</sub> removal efficiency. This trend can be explained based on the CO<sub>2</sub> loading values (see Fig. 10). For Cases 2 and 3 the CO<sub>2</sub> loading in the PSA gas systems increases which result in the reduction of regeneration heat. In a comparison of the regeneration heat of Cases 1 to 3, it is the highest for Case 1 followed by Case 2 and the least is observed in Case 3. This can be explained as; in the CO<sub>2</sub>-MEA absorption system, the regeneration heat decreases as the CO<sub>2</sub> loading increases above 0.5 mol/mol. This is because of the significant reduction in the heat of reaction related to carbamate reversion and CO<sub>2</sub> hydration reactions (Xu, 2011). In Case 1, as the CO<sub>2</sub> loading is limited to 0.5 mol/mol due to the lower CO<sub>2</sub> partial pressures therefore the regeneration heat is the highest. In Case 3, the CO<sub>2</sub> loading reaches 0.62

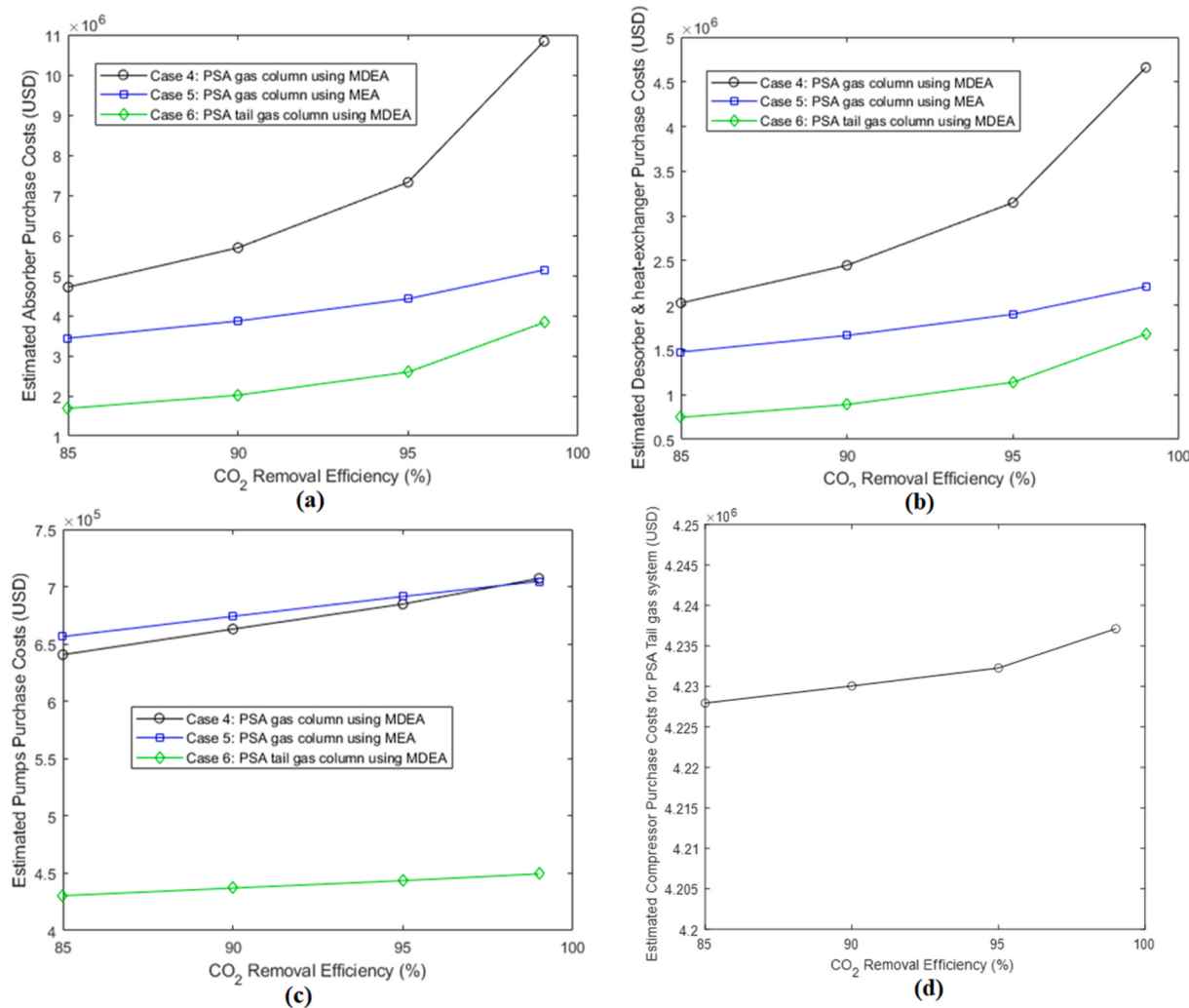


Fig. 17. Estimated purchase costs for Cases 4 to 6.

mol/mol which results in the reduction of regeneration heat and is found to be the lowest.

The economic evaluation for the described Cases 1–3 has been illustrated in Figs. 12–14. The estimated total purchase cost of the main absorption process equipment includes, absorbers, desorbers, a main heat exchanger (rich-lean solvent), lean and rich solvent pumps, and a blower. In Fig. 12 (a), in general the purchase cost increases as the CO<sub>2</sub> removal efficiency increases for Cases 1 to 3, with the most significant effect of an absorber and a desorber purchase costs. Heat exchanger cost is included in desorber for simplicity. Among all cases, the highest absorber purchase cost is observed to be for the absorber column used for PSA gas stream due to the larger column diameter and relatively thick wall in comparison to absorber column used for the flue gas stream. Fig. 12 (c) shows the estimated total purchase costs of pumps, it can be observed that it slightly increases with the CO<sub>2</sub> removal efficiency. This is mainly because of the increasing required head as the result of higher column heights. Further, in the comparison of Cases 1 to 3, the highest pump cost is found to be for Case 2 because of the requirement of relatively high total solvent flow rates and higher heads in comparison to Case 1 due to high column operating pressures in the PSA gas column. The blower is required with the flue gas column to maintain the column pressure. In Fig. 12 (d), the trend of the blower purchase cost is shown as a function of CO<sub>2</sub> removal efficiencies, it is seen that the cost of the blower used in Case 1 is highest because of the highest gas load. In Cases 2 and 3, the blower cost is lower because the total plant CO<sub>2</sub> is partially removed at the PSA inlet gas stream, so it

reduces the gas load at the blower of reformer flue gas absorber. In addition, it is also seen that in Cases 2 and 3, the purchasing cost is slightly reduced with the CO<sub>2</sub> removal efficiency, this is because the higher percentage of CO<sub>2</sub> is removed from the PSA gas stream and the remaining separation load decreases in the flue gas column section.

The yearly operating cost of the main equipment including pumps, and blowers are estimated in terms of the electricity cost, whereas the reboiler duty is estimated using the steam cost as shown in Fig. 13 (a)–(c). It can be observed that in general the trends of the operating costs also reflect the equipment purchase cost because mainly the required load controls both the purchase and operating costs. Similarly, the steam cost reflects the profiles of regeneration heat requirements as shown earlier in Fig. 10 (d). It is to note that steam cost is the main contributor for the cost-effectiveness economy of the absorption process. In a comparison of Cases 1 to 3, Case 3 consumes minimum steam due to the operation in the high CO<sub>2</sub> loading region as explained earlier in the section.

The overall comparison of Cases 1 to 3 can effectively be viewed using the comparison of overall capital, operating and annualized operating costs. Therefore, Fig. 14 (a) shows the effect of CO<sub>2</sub> removal efficiency on the total capital cost. It is revealed that the capital cost for Case 3 is maximum and for Case 1 is minimum due to the simpler plant design. However, the capital cost of Case 3 is slightly higher than Case 2 although in Case 2 two desorber units are required, this is mainly due to the larger absorber required in the PSA gas system as described earlier. The total operating cost is shown in Fig. 14 (b) which shows that no

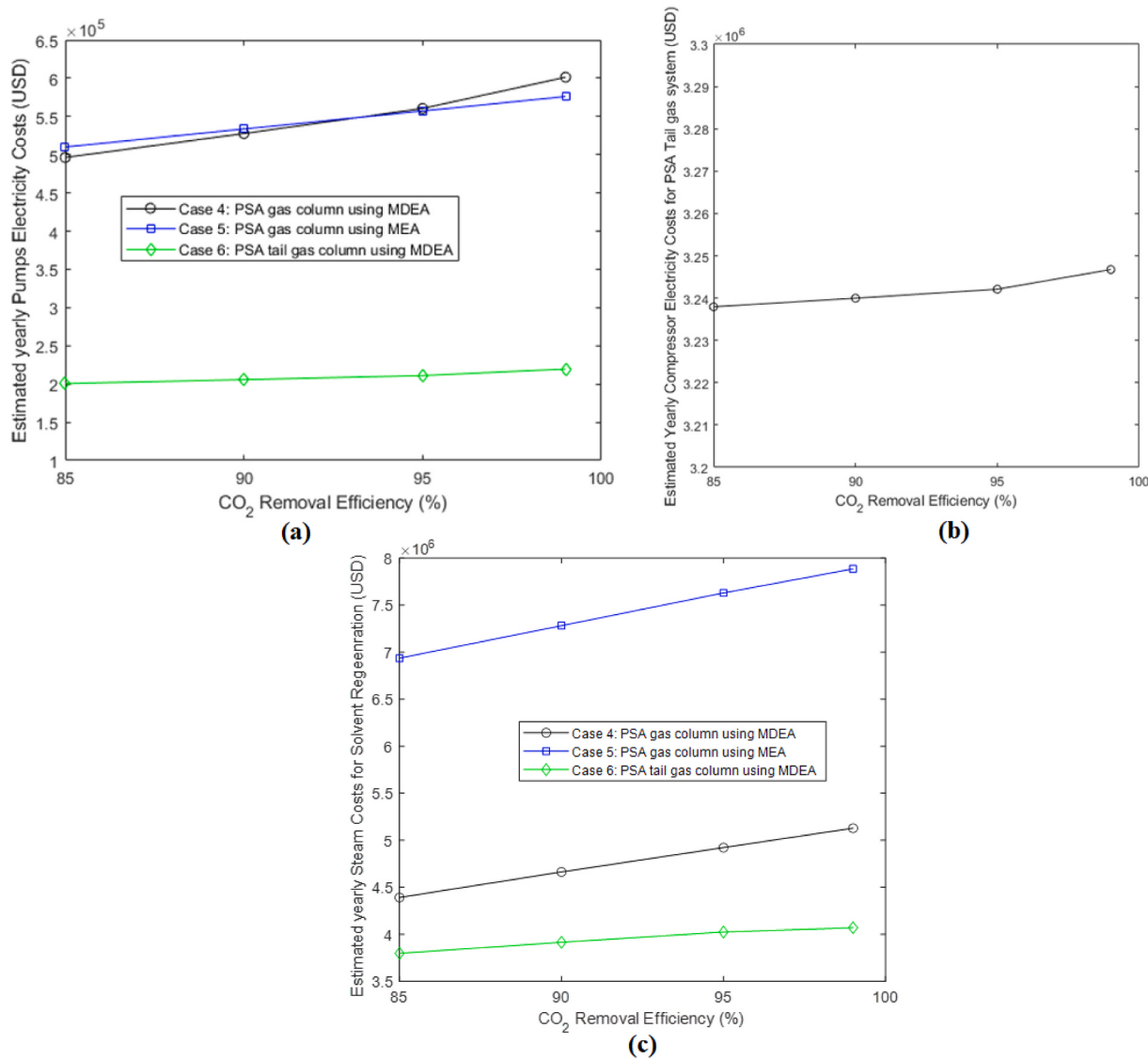


Fig. 18. Estimated operating costs for Cases 4 to 6.

considerable impact of CO<sub>2</sub> removal efficiency on the total operating cost is observed. This is because although the electricity requirement increases for the pump but on the other hand steam requirement slightly decreases due to the higher CO<sub>2</sub> loadings. As it has been explained earlier that with the increment of CO<sub>2</sub> loadings, the regeneration heat decreases and eventually the steam requirements. Finally, Cases 1 to 3 are compared for the five years annualized cost which reveals that Case 3 is the most economic among all. This is mainly attributed to the requirement of relatively lower energy cost for solvent regeneration.

#### 6.4. Results of cases with partial CO<sub>2</sub> removal (Cases 4 to 6)

In this section, the evaluation of process design and economic factors is presented for Cases 4 to 6 in a similar approach as has been given earlier. Fig. 15 (a)-(d) show the effect of CO<sub>2</sub> removal efficiency on the process design variables including, packing height, column diameter, required solvent, and solvent regeneration heat. It can be observed that the required packing heights have not been significantly affected by increasing CO<sub>2</sub> removal efficiency. This is mainly because Cases 4 to 6 are operated at high pressures and the required solvent flowrates are increased with CO<sub>2</sub> removal rate as shown in Fig. 15 (c), with more or less the same CO<sub>2</sub> loading as shown in Fig. 16. Fig. 15 (d) shows

regeneration heat as a function of CO<sub>2</sub> removal efficiency. It can be observed that the required heat is almost constant for the observed range of CO<sub>2</sub> removal efficiency due to similar CO<sub>2</sub> loading conditions.

The purchase cost estimation for Cases 4 to 6 is shown using Fig. 17 (a) to (c). It can be observed that the estimated purchase cost for the absorber is the highest for Case 4 due to higher column height. Case 5 requires lower purchase cost due to the relatively lower packing height and Case 6 is the lowest column cost due to relatively smaller column diameter. The total purchase cost of desorber and heat exchanger show similar profiles for Cases 4 to 6 as that of the absorber purchase costs. This is because the purchase costs of the desorber and heat exchanger are correlated to the purchase cost of the absorber as shown in Eqs. (34) and (35). The purchase cost of pumps for Cases 4 and 5 is higher than Case 6 mainly because of the higher operating pressure and the solvent flowrates. In comparison to Cases 4 and 5 the purchase cost of pumps is nearly the same due to the more or less same required heads. In Case 6, the compressor is also used and therefore the purchase costs are shown in Fig. 17 (d). It shows that compressor cost slightly increases as the CO<sub>2</sub> removal efficiency increases due to the variation in gas density.

The operating costs estimation for Cases 4 to 6 in terms of the electricity cost for pumps, and compressors are respectively shown in Fig. 18 (a) and (b). The pumping electricity cost profiles for Cases 4 to 6 reflects

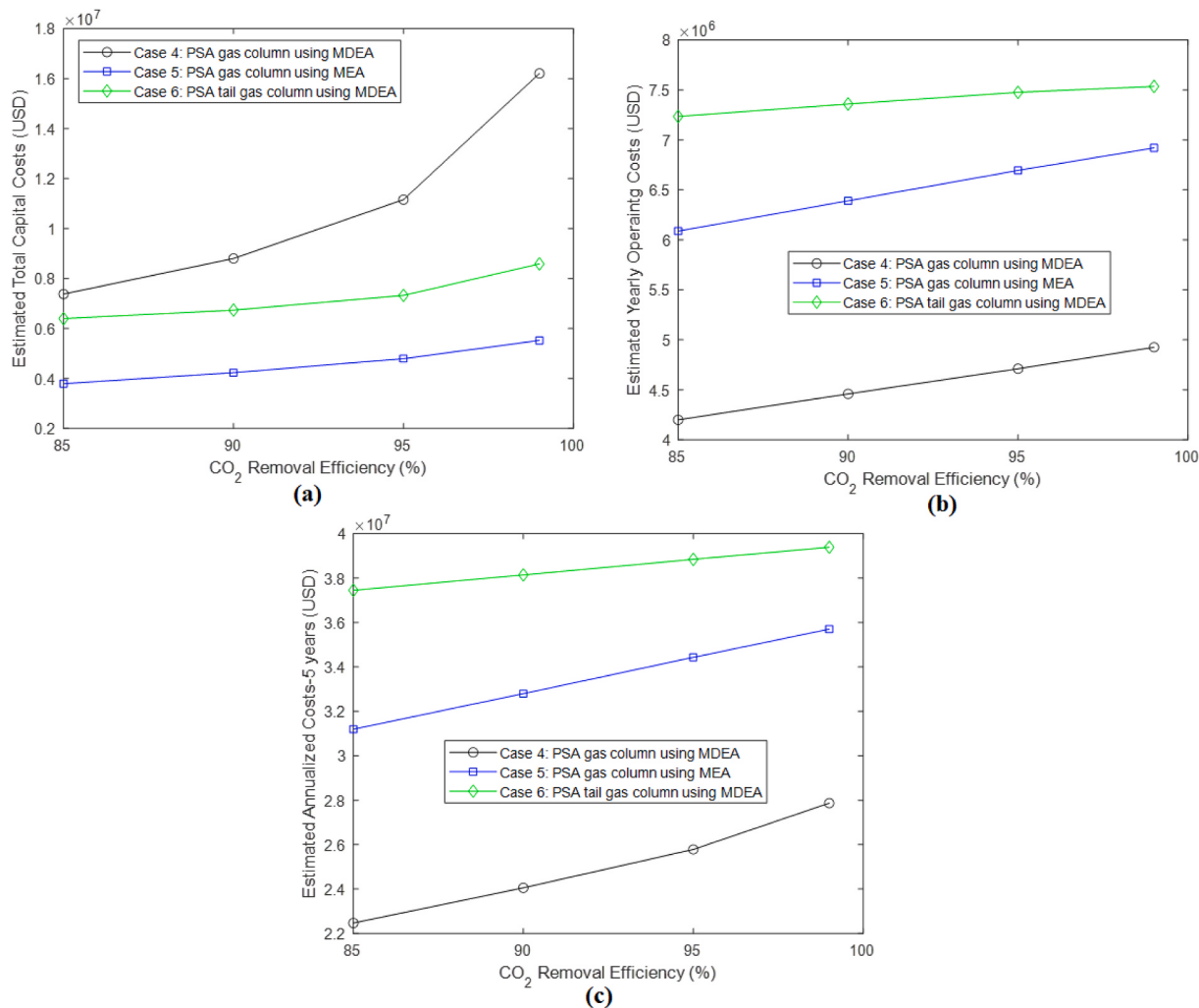


Fig. 19. Total capital, operating and annualized costs for Cases 4 to 6.

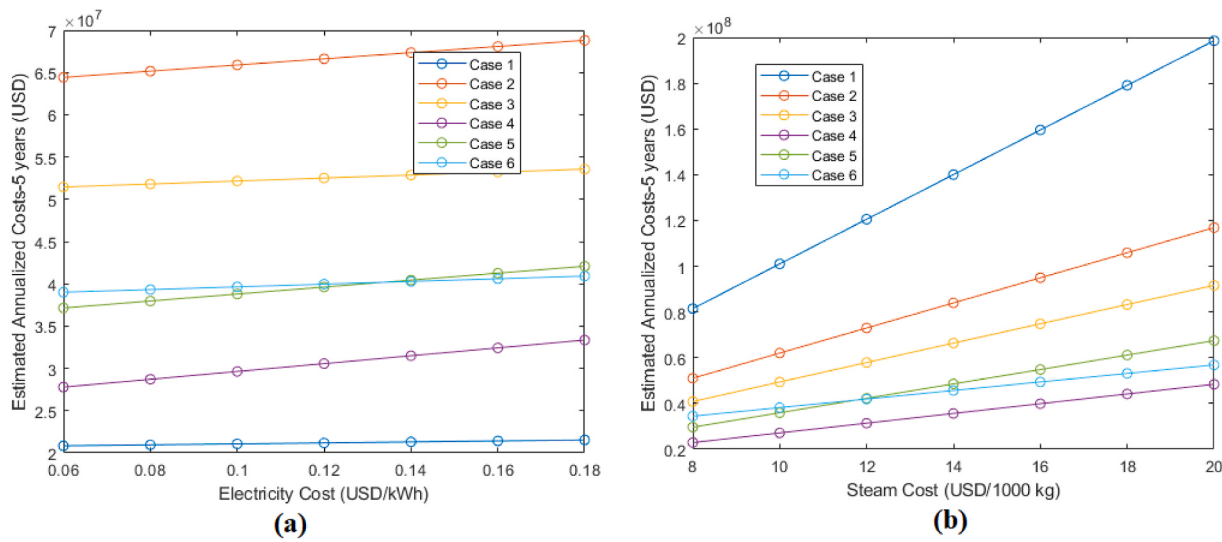


Fig. 20. Sensitivity analysis: (a) Electricity unit cost (b) Steam unit cost.

their respective purchase costs profiles because both depend on the required loads. Similarly, the profile of compression electricity cost is also comparable to that of the compressor purchase cost. Fig. 18 (c)

shows annual cost related to steam consumption for Cases 4 to 6 which mainly depends upon the required heat duty to regenerate a solvent. Thereby the ranking of the illustrated cases is similar in order of their

respective required solvent regeneration heats as shown earlier in Fig. 15(d).

To conclude the performance of Cases 3 to 4, the total capital, operating and five years annualized costs are compared in Fig. 19 (a)-(c). It is revealed that Case 4 shows the highest capital cost due to the larger column sizes but offers the lowest operating costs mainly due to the relatively lower steam requirements. Case 5 offers relatively lower total capital costs in comparison to Case 4 due to the lower absorber size. However, it needs relatively higher operating costs because of the high regeneration heats required for the MEA system. Case 6 shows the highest annualized cost mainly due to the highest operating cost in result of the additional compression requirements. Cases 4 and 5 are presented in IEAGHG report (IEAGHG, 2017) for the detailed economic analysis which reveals that Case 6 is more expensive than Case 4 because of both the higher capital and operating costs. In the present study, although Case 6 is more expensive than Case 5 in terms of operating costs and annualized cost, it is seen that Case 6 shows slightly lower capital cost in comparison to Case 5 (90% efficiency). This difference is thought as in this study higher MDEA concentration (50%) is used for PSA tail gas which eventually decreases the required column size.

### 6.5. Sensitivity analysis

The estimated 5- years annualized cost of Cases 1–6 have been evaluated by varying electricity and steam unit cost as shown in Fig. 20 (a) and (b). It can be observed that the estimated annualized cost linearly increases for all the cases as the electricity unit cost increases. The increasing rate of Cases 1–6 are slightly different because of the difference in the electricity consumption for pumping and compression operations. Cases 2 and 3 demands more pumping in comparison to Case 1, leading to higher increasing rate. Similarly, the estimated 5-year annualized cost for Case 5 exceeds Case 6 around 0.18 USD/kWh electricity cost because of the higher pumping requirements due to higher required heads. In comparison to electricity cost effect, steam unit cost significantly effects the estimated 5-year annualized cost of all the cases. The increasing trend is observed to be linear with the highest observation in Case 1 because of highest regeneration heat requirements. For Case 5 the increasing rate is also quite high and exceeds Case 6 due to the higher regeneration heat requirements.

## 7. Conclusion

The amine-based chemical absorption process is a well-known technology to integrate with the SMR plant to capture CO<sub>2</sub>. It can be coupled with any of the three available gas streams including, reformer flue gas, PSA inlet and tail gas streams. In this study, an amine-based chemical absorption process has been applied to capture CO<sub>2</sub> from the SMR-based hydrogen production plant using multiple options, including single and dual absorption plants and solvents (MEA and MDEA) as well. Moreover, a novel process design approach based on the arrangements for the simultaneous removal of CO<sub>2</sub> from flue gas and the PSA inlet gas stream is proposed, in which a single solvent (MEA) can be used to treat both the flue gas and PSA gas streams simultaneously. The rate-based model has been implemented in the MATLAB environment to simulate the absorption process to evaluate the effect of required CO<sub>2</sub> removal efficiency on packing heights, column diameter, and solvent flow rates. The solvent regeneration energies are also estimated by computing the heat of reaction, vaporization, and sensible heat. The techno-economic analysis at the conceptual level has been presented to compare the multiple described Cases (1–6). The conclusions drawn in this study are as follows:

1. It is found that the packing height of the absorber plays the most important role in the capital cost of the absorption process whereas the regeneration heat requirements control the operating costs.

2. The estimated annualized cost is found to be increased as the CO<sub>2</sub> removal efficiency is increased from 85 to 99%, mainly due to the increase of absorber size and so the capital costs.
3. Based on the conventional methods, to capture nearly 100% of the total plant CO<sub>2</sub>, in comparison to the single plant option (Case 1) the option of using two plants (Case 2) is found to be more economical. The estimated annualized cost of Case 2 is relatively 36.7% less in comparison to Case 1. This is mainly due to the significantly lower required solvent regeneration costs of Case 2.
4. The estimated annualized cost of the novel proposed method (Case 3) is found as 48% and 17.9% less in the relative comparison to Case 1 and Case 2. This is due to the relatively lower solvent regeneration cost.
5. In the comparison of partial CO<sub>2</sub> removal Cases (4–6), Case 4 which is the established conventional method found to be 35.3% and 24.4% less expensive in terms of the estimated annualized costs respectively for Cases 5 and 6. This is because in Case 5 relatively large regeneration heat is required whereas in Case 6 additional compressional costs are required.

For the future work, the presented novel method will be further evaluated using the comprehensive process simulation and economic analysis. Moreover, the other potential amine solvent combinations such as MDEA-PZ or MDEA-MEA will be evaluated.

### CRediT authorship contribution statement

**Muhammad Zubair Shahid:** Conceptualization, Methodology, Investigation, Validation, Software, Writing – original draft. **Jin-Kuk Kim:** Methodology, Investigation, Validation, Writing – review & editing.

### Declaration of competing interest

The authors declare that they have no known competing financial interests or personal relationships that could have appeared to influence the work reported in this paper.

### Data availability

The data used in the study are included in the manuscript.

### Acknowledgements

This work was supported by the National Research Foundation of Korea (NRF) (2019R1A2C2002263, 2022 R1A5A1032539) funded by the Korean Government (MSIT) and by the Korea Institute of Energy Technology Evaluation and Planning (KETEP) funded by the Ministry of Trade, Industry and Energy (MOTIE) (No. 20224C10300050).

### Appendix A. Supplementary data

Supplementary data to this article can be found online at <https://doi.org/10.1016/j.jclepro.2023.136704>.

### Nomenclature

$a_e$	effective packing area (m <sup>2</sup> /m <sup>3</sup> )
$A_{nc}$	annualized cost (USD)
$a_p$	total packing area (m <sup>2</sup> /m <sup>3</sup> )
$C_A$	molar concentration of component A (kmol/m <sup>3</sup> )
$C_{op}$	total annual operating cost (USD)
$C_p$	purchase cost (USD)
$C_{pi}$	heat capacity of component i, i = CO <sub>2</sub> and H <sub>2</sub> O (J/kmol K)
CR	concentration of MEA or MDEA (m <sup>2</sup> /s)
$D_C$	column diameter (m)

$D_{CO2l}$	diffusivity of CO <sub>2</sub> in liquid phase (m <sup>2</sup> /s)
$D_R$	diffusivity of reactant (MEA or MDEA) (m <sup>2</sup> /s)
$E$	enhancement factor, dimensionless
$E_w$	fractional welding efficiency
$f_{CO2}$	partial fugacity of CO <sub>2</sub> in bulk phase (atm)
$f_{CO2i}$	partial fugacity of CO <sub>2</sub> at gas-liquid interface (atm)
$F_M$	material type factor
$F_{TM}$	motor type factor
$F_{TP}$	pump type factor
$G$	total gas flow rate (mol/s)
$H$	Henry Law constant (kmol/m <sup>3</sup> atm)
$H_R$	enthalpy of reaction (kJ/mol)
$H_V$	enthalpy of vaporization (kJ/mol)
$k^o_L$	liquid phase mass transfer coefficient without reaction (m/s)
$k_2$	second order rate constant (m <sup>3</sup> /kmol s)
$k_G$	gas phase mass transfer coefficient (kmol/atm m <sup>2</sup> s)
$k_L$	liquid phase mass transfer coefficient (m/s)
$L$	liquid phase flow rate (m <sup>3</sup> /m <sup>2</sup> h)
$L_C$	column length (m)
$M$	Hatta number, dimensionless
$N_{CO2}$	molar flux of CO <sub>2</sub> gas (kmol/m <sup>2</sup> s)
$P$	pressure (atm)
$QR$	heat of reaction (kJ/mol)
$Q_{reg}$	heat of solvent regeneration (kJ/kg CO <sub>2</sub> )
$Q_s$	sensible heat (kJ/mol)
$Q_V$	heat of vaporization (kJ/mol)
$S$	allowable stress
$S$	pump size factor
$T_G$	gas temperature (K)
$T_L$	liquid temperature (K)
$t_s$	column wall thickness (m)
$W$	weight of Vessel (kg)
$x_{CO2}$	mole fraction of CO <sub>2</sub> in a liquid phase
$y_{CO2}$	mole fraction of CO <sub>2</sub> in a gas phase
$Z$	packing height (m)
<b>Greek Symbols</b>	
$\rho$	density (kg/m <sup>3</sup> )
$\Phi$	fugacity coefficient
$\eta$	equipment efficiency
$\alpha_{Lean}$	CO <sub>2</sub> loading of lean solvent
<b>References</b>	
Aboudheir, A., Tontiwachwuthikul, P., Chakma, A., Idem, R., 2003. Kinetics of the reactive absorption of carbon dioxide in high CO <sub>2</sub> loaded, concentrated aqueous monoethanolamine solutions. <i>Chem. Eng. Sci.</i> 58 (23–24), 5195–5210.	
Ali, H., Eldrup, N.H., Normann, F., Skagestad, R., Øi, L.E., 2019. Cost estimation of CO <sub>2</sub> absorption plants for CO <sub>2</sub> mitigation—method and assumptions. <i>Int. J. Greenh. Gas Control</i> 88, 10–23.	
Ali Khan, M.H., Daiyan, R., Neal, P., Haque, N., MacGill, I., Amal, R., 2021. A framework for assessing economics of blue hydrogen production from steam methane reforming using carbon capture storage & utilisation. <i>Int. J. Hydrogen Energy</i> 46 (44), 22685–22706.	
Antonini, C., Pérez-Calvo, J.-F., Van Der Spek, M., Mazzotti, M., 2021. Optimal design of an MDEA CO <sub>2</sub> capture plant for low-carbon hydrogen production—a rigorous process optimization approach. <i>Separ. Purif. Technol.</i> 279, 119715.	
Aromada, S.A., Eldrup, N.H., Normann, F., Øi, L.E., 2020. Techno-economic assessment of different heat exchangers for co <sub>2</sub> capture. <i>Energies</i> 13 (23), 6315.	
Atilhan, S., Park, S., El-Halwagi, M.M., Atilhan, M., Moore, M., Nielsen, R.B., 2021. Green hydrogen as an alternative fuel for the shipping industry. <i>Curr. Opin. Chem. Eng.</i> 31, 100668.	
Billet, R., Schultes, M., 1993. Predicting mass transfer in packed columns. <i>Chem. Eng. Technol.: Indust. Chem. Plant Equip. Process Eng. Biotechnol.</i> 16 (1), 1–9.	
Capurso, T., Stefanizzi, M., Torresi, M., Camporeale, S.M., 2022. Perspective of the role of hydrogen in the 21st century energy transition. <i>Energy Convers. Manag.</i> 251, 114898.	
Collodi, G., 2010. Hydrogen production via steam reforming with CO <sub>2</sub> capture. <i>Chem. Eng. Transact.</i> 19, 37–42.	
Edwards, T., Maurer, G., Newman, J., Prausnitz, J., 1978. Vapor-liquid equilibria in multicomponent aqueous solutions of volatile weak electrolytes. <i>AIChE J.</i> 24 (6), 966–976.	
Ellaf, A., Taqvi, S.A.A., Zaeem, D., Siddiqui, F.U.H., Kazmi, B., Idris, A., Alshgari, R.A., Mushab, M.S.S.J.C., 2023. Energy, exergy, economic, environment, exergoenvironment based assessment of amine-based hybrid solvents for natural gas sweetening, 313, 137426.	
Haji-Sulaiman, M., Aroua, M.K., Benamor, A., 1998. Analysis of equilibrium data of CO <sub>2</sub> in aqueous solutions of diethanolamine (DEA), methyldiethanolamine (MDEA) and their mixtures using the modified Kent Eisenberg model. <i>Chem. Eng. Res. Des.</i> 76 (8), 961–968.	
Hulst, N.v., 2019. The Clean Hydrogen Future Has Already Begun. IEA, Paris.	
IEA, 2020. Energy Technology Perspectives 2020. IEA, Paris.	
IEAGHG, 2017. Techno-Economic Evaluation of SMR Based Standalone (Merchant) Plant with CCS, 2017/0.2, February.	
IPCC, 2018. Climate Change and Land: an IPCC Special Report on Climate Change.	
Junsittiwe, R., Srinophakun, T.R., Sukpancharoen, S., 2022. Techno-economic, environmental, and heat integration of palm empty fruit bunch upgrading for power generation. <i>Energy Sustain. Develop.</i> 66, 140–150.	
Khalifa, O., Alkhatab, I.I., Bahamon, D., Alhajaj, A., Abu-Zahra, M.R., Vega, L.F., 2022. Modifying absorption process configurations to improve their performance for Post-Combustion CO <sub>2</sub> capture—What have we learned and what is still Missing? <i>Chem. Eng. J.</i> 430, 133096.	
Meerman, J.C., Hamborg, E.S., van Keulen, T., Ramírez, A., Turkenburg, W.C., Faaij, A.P.C., 2012. Techno-economic assessment of CO <sub>2</sub> capture at steam methane reforming facilities using commercially available technology. <i>Int. J. Greenh. Gas Control</i> 9, 160–171.	
Nazir, S.M., Cloete, J.H., Cloete, S., Amini, S., 2019. Efficient hydrogen production with CO <sub>2</sub> capture using gas switching reforming. <i>Energy</i> 185, 372–385.	
Noussan, M., Raimondi, P.P., Scita, R., Hafner, M., 2021. The role of green and blue hydrogen in the energy transition—A technological and geopolitical perspective, 13 (1), 298.	
Nwoaha, C., Saiwan, C., Supap, T., Idem, R., Tontiwachwuthikul, P., Al-Marri, M.J., Benamor, A., 2017. Regeneration energy analysis of aqueous tri-solvent blends containing 2-amino-2-methyl-1-propanol (AMP), methyldiethanolamine (MDEA) and diethylenetriamine (DETA) for carbon dioxide (CO <sub>2</sub> ) capture. <i>Energy Proc.</i> 114, 2039–2046.	
Onda, K., Takeuchi, H., Okumoto, Y., 1968. Mass transfer coefficients between gas and liquid phases in packed columns. <i>J. Chem. Eng. Jpn.</i> 1 (1), 56–62.	
Pellegrini, L.A., De Guido, G., Moioli, S., 2020. Design of the CO <sub>2</sub> removal section for PSA tail gas treatment in a hydrogen production plant. <i>Front. Energy Res.</i> 8.	
Posey, M.L., Tapperson, K.G., Rochelle, G.T., 1996. A simple model for prediction of acid gas solubilities in alkanolamines. <i>Gas Separ. Purif.</i> 10 (3), 181–186.	
Roussanaly, S., Anantharaman, R., Fu, C., 2020. Low-carbon footprint hydrogen production from natural gas: a techno-economic analysis of carbon capture and storage from steam-methane reforming. <i>Chem. Eng. Transact.</i> 81, 1015–1020.	
Seider, W.D., Seader, J.D., Lewin, D.R., 2009. <i>PRODUCT &amp; PROCESS DESIGN PRINCIPLES: SYNTHESIS, ANALYSIS AND EVALUATION</i> , (With CD). John Wiley & Sons.	
Shahid, M.Z., Maulud, A.S., Azmi Bustam, M., Suleman, H., 2020. Modeling of CO <sub>2</sub> -MEA absorption system in the packed column using Sulzer DX structured packing. <i>IOP Conf. Ser. Mater. Sci. Eng.</i> 736 (2), 022059.	
Shahid, M.Z., Maulud, A.S., Bustam, M.A., Suleman, H., Abdul Halim, H.N., Shariff, A.M., 2021. Packed column modelling and experimental evaluation for CO <sub>2</sub> absorption using MDEA solution at high pressure and high CO <sub>2</sub> concentrations. <i>J. Nat. Gas Sci. Eng.</i> 88, 103829.	
Shahid, M.Z., Maulud, A.S., Bustam, M.A., Suleman, H., Halim, H.N.A., Shariff, A.M., 2019. Rate-based modeling for packed absorption column of the MEA–CO <sub>2</sub> –water system at high-pressure and high-CO <sub>2</sub> loading conditions. <i>Ind. Eng. Chem. Res.</i> 58 (27), 12235–12246.	
Soltani, R., Rosen, M., Dincer, I., 2014. Assessment of CO <sub>2</sub> capture options from various points in steam methane reforming for hydrogen production. <i>Int. J. Hydrogen Energy</i> 39 (35), 20266–20275.	
Soltani, S.M., Lahiri, A., Bahzad, H., Clough, P., Gorbounov, M., Yan, Y., 2021. Sorption-enhanced steam methane reforming for combined CO <sub>2</sub> capture and hydrogen production: a state-of-the-art review. <i>Carbon Capture Sci. Technol.</i> 1, 100003.	
Song, H.-J., Lee, S., Park, K., Lee, J., Chand Spah, D., Park, J.-W., Filburn, T.P., 2008. Simplified estimation of regeneration energy of 30 wt% sodium glycinate solution for carbon dioxide absorption. <i>Ind. Eng. Chem. Res.</i> 47 (24), 9925–9930.	
Song, H., Liu, Y., Bian, H., Shen, M., Lin, X., 2022. Energy, environment, and economic analyses on a novel hydrogen production method by electrified steam methane reforming with renewable energy accommodation. <i>Energy Convers. Manag.</i> 258, 115513.	
Suleman, H., Maulud, A.S., Fosbøl, P.L., Nasir, Q., Nasir, R., Shahid, M.Z., Nawaz, M., Abunawara, M., 2021. A review of semi-empirical equilibrium models for CO <sub>2</sub> -alkanolamine-H <sub>2</sub> O solutions and their mixtures at high pressure. <i>J. Environ. Chem. Eng.</i> 9 (1), 104713.	
Suleman, H., Maulud, A.S., Man, Z., 2015. Review and selection criteria of classical thermodynamic models for acid gas absorption in aqueous alkanolamines. <i>Rev. Chem. Eng.</i> 31 (6), 599–639.	
Tan, L., Shariff, A., Lau, K., Bustam, M., 2015. Impact of high pressure on high concentration carbon dioxide capture from natural gas by monoethanolamine/N-methyl-2-pyrrolidone solvent in absorption packed column. <i>Int. J. Greenh. Gas Control</i> 34, 25–30.	
The-Paris-Agreement-2021, The Paris Agreement 2021.	
Tontiwachwuthikul, P., Meisen, A., Lim, C.J., 1992. CO <sub>2</sub> absorption by NaOH, monoethanolamine and 2-amino-2-methyl-1-propanol solutions in a packed column. <i>Chem. Eng. Sci.</i> 47 (2), 381–390.	

- van der Spek, M., Banet, C., Bauer, C., Gabrielli, P., Goldthorpe, W., Mazzotti, M., Munkejord, S.T., Røkke, N.A., Shah, N., Sunny, N., 2022. Perspective on the hydrogen economy as a pathway to reach net-zero CO<sub>2</sub> emissions in Europe. *Energy Environ. Sci.* 15 (3), 1034–1077.
- Vega, F., Baena-Moreno, F.M., Gallego Fernández, L.M., Portillo, E., Navarrete, B., Zhang, Z., 2020. Current status of CO<sub>2</sub> chemical absorption research applied to CCS: towards full deployment at industrial scale. *Appl. Energy* 260, 114313.
- Voldsgård, M., Jordal, K., Anantharaman, R., 2016. Hydrogen production with CO<sub>2</sub> capture. *Int. J. Hydrogen Energy* 41 (9), 4969–4992.
- Wellek, R., Brunson, R., Law, F., 1978. Enhancement factors for gas-absorption with second-order irreversible chemical reaction. *Can. J. Chem. Eng.* 56 (2), 181–186.
- Xu, Q., 2011. Thermodynamics of CO<sub>2</sub> Loaded Aqueous Amines. University of Texas.
- Younas, M., Shafique, S., Hafeez, A., Javed, F., Rehman, F., 2022. An overview of hydrogen production: current status, potential, and challenges. *Fuel* 316, 123317.
- Yun, S., Jang, M.-G., Kim, J.-K., 2021. Techno-economic assessment and comparison of absorption and membrane CO<sub>2</sub> capture processes for iron and steel industry. *Energy* 229, 120778.
- Yun, S., Oh, S.-Y., Kim, J.-K., 2020. Techno-economic assessment of absorption-based CO<sub>2</sub> capture process based on novel solvent for coal-fired power plant. *Appl. Energy* 268, 114933.